DMD Fast Forward. Published on June 1, 2020 as DOI: 10.1124/dmd.120.090670
This article has not been copyedited and formatted. The final version may differ from this version.

Absorption and Disposition of Coproporphyrin I (CPI) in Cynomolgus Monkeys and Mice: Pharmacokinetic Evidence to Support the Use of CPI to Inform the Potential for OATP Inhibition

Xiaomei Gu, Lifei Wang, Jinping Gan, R. Marcus Fancher, Yuan Tian, Yang Hong, Yurong Lai, Michael Sinz, and Hong Shen

Departments of Metabolism and Pharmacokinetics (X.G., L.W., J.G., R.M.F., Y.L., M.S., and H.S.) and Radiochemistry (Y.T. and Y.H.), Bristol-Myers Squibb Company, Route 206 & Province Line Road, Lawrenceville, NJ 08543

Downloaded from dmd.aspetjournals.org at ASPET Journals on April 18, 2024

DMD Fast Forward. Published on June 1, 2020 as DOI: 10.1124/dmd.120.090670
This article has not been copyedited and formatted. The final version may differ from this version.

Running Title: Absorption and disposition of CP in monkeys and mice

Corresponding authors and contact information:

Dr. Hong Shen

The Department of Metabolism and Pharmacokinetics (MAP), Bristol-Myers Squibb Company

Route 206 & Province Line Road, Lawrenceville, NJ 08543

E-mail: hong.shen1@bms.com

Phone: 609-252-4509

Downloaded from dmd.aspetjournals.org at ASPET Journals on April 18, 2024

Number of text pages: 28

Number of tables: 6

Number of figures: 7

Number of references: 59

Number of words:

Abstract: 251

Introduction: 1,121

Discussion: 1,714

Abbreviations: ADME, absorption, distribution, metabolism, and elimination; *AUC*, area under the plasma concentration-time curve; *AUCR*, area under the plasma-time curve fold change; C_{max}, maximum plasma concentration; CPI, coproporphyrin I; CPI-d8, octadeuterium-labeled coproporphyrin I; CPIII, coproporphyrin III; CsA, cyclosporin A; DDI, drug-drug interaction;

DMD Fast Forward. Published on June 1, 2020 as DOI: 10.1124/dmd.120.090670
This article has not been copyedited and formatted. The final version may differ from this version.

FSM, furosemide; IC_{50}, concentration required to inhibit transport by 50%; LC-MS/MS, liquid chromatography–tandem mass spectrometry; MATE, multidrug and toxin extrusion protein; MFM, metformin; NCE, new chemical entity; NTCP, sodium taurocholate cotransporting polypeptide; OAT, organic anion transporter; OCT, organic cation transporter; OATP, organic anion-transporting polypeptide; PROB, probenecid; PYR, pyrimethamine; QWBA, quantitative whole-body autoradiography; RIF, rifampicin; SD, standard deviation.

Downloaded from dmd.aspetjournals.org at ASPET Journals on April 18, 2024

DMD Fast Forward. Published on June 1, 2020 as DOI: 10.1124/dmd.120.090670
This article has not been copyedited and formatted. The final version may differ from this version.

ABSTRACT

Despite a recent expansion in the recognition of coproporphyrin's (CP's) potential utility as an endogenous biomarker of OATP1B activity, there have been few detailed studies of CP's pharmacokinetic behavior and an overall poor understanding of its pharmacokinetic fate from tissues and excretion. Here, we describe the pharmacokinetics of deuterium-labeled coproporphyrin I (CPI-d8) in cynomolgus monkeys following oral and intravenous administration. CPI-d8 has a half-life and bioavailability of 7.6 h and 3.2%, respectively. Cynomolgus monkeys received oral cyclosporin A (CsA) at 4, 20, and 100 mg/kg which yielded maximum blood concentrations (C_{max}) and area under the plasma concentration-time curve (*AUC*) values of 0.19, 2.5, and 3.8 μM, and 2.7, 10.5, and 26.6 μM●h, respectively. The apparent CsA-dose dependent increase in the *AUC* ratio (*AUCR*) of CPI-d8 (1.8, 6.2, and 10.5), CPI (1.1, 1.4, and 4.4), and CPIII (1.1, 1.8, and 4.6) at 4, 20, and 100 mg, respectively. In contrast, the plasma concentrations of CPI and CPIII were generally not affected by IV administration of the renal organic anion and cation transporter inhibitors [probenecid (PROB) and pyrimethamine (PYR), respectively]. In addition, tritium-labeled coproporphyrin I ([^{3}H]CPI) showed specific and rapid distribution to the liver, intestine, and kidney after an IV dose in mice using quantitative whole-body autoradiography (QWBA). Rifampin (RIF) markedly reduced the liver and intestinal uptake of ([^{3}H]CPI) while increasing the kidney uptake. Taken together, these results suggest that hepatic OATP considerably affects the disposition of CPI in animal models, indicating CPI is a sensitive and selective endogenous biomarker of OATP inhibition.

Downloaded from dmd.aspetjournals.org at ASPET Journals on April 18, 2024

DMD Fast Forward. Published on June 1, 2020 as DOI: 10.1124/dmd.120.090670
This article has not been copyedited and formatted. The final version may differ from this version.

SIGNIFICANCE STATEMENT

This study demonstrated that CPI has favorable oral absorption, distribution, and elimination profiles in monkeys and mice as an endogenous biomarker. It also demonstrated its sensitivity and selectivity as a probe of OATP1B activity. The study reports, for the first time, in vivo pharmacokinetics, tissue distribution, sensitivity, and selectivity of CPI as an OATP1B endogenous biomarker in animals. The data provides preclinical support for exploration of its utility as a sensitive and selective circulating OATP biomarker in humans.

Downloaded from dmd.aspetjournals.org at ASPET Journals on April 18, 2024

DMD Fast Forward. Published on June 1, 2020 as DOI: 10.1124/dmd.120.090670
This article has not been copyedited and formatted. The final version may differ from this version.

INTRODUCTION

Although most of the observed drug-drug interactions (DDIs) are caused by CYP3A inhibition and induction when developing a new drug, drug transporters also play an important role in drug interactions. Either alone or with a drug-metabolizing enzyme, they mediate approximately half of all DDIs characterized in the package inserts of 34 new small molecule drugs that were approved by the United States Food and Drug Administration (FDA) in 2017 (Yu et al., 2019). Moreover, hepatic organic anion-transporting polypeptides (OATP)1B1 and OATP1B3 mediated more than half of the DDIs with area under the plasma-time curve fold change (*AUCR*) greater than or equal to 5 (Yu et al., 2019). In agreement, the OATP/Oatp transporters are the most abundant transporter proteins, accounting for 29 to 69% of total drug transporter proteins in the liver across species (Wang et al., 2015). Furthermore, the observed individual and interethnic variability in OATP1B1 transport activity has been demonstrated to be a cause of variability in pharmacokinetics, efficacy and safety of OATP1B drug substrates (Marzolini et al., 2004, Konig et al., 2006, Group et al., 2008, Tomita et al., 2013). Consequently, the *in vitro* and *in vivo* approaches to assess the inhibition potential of a new drug towards OATP1B1 and OATP1B3 have been recommended and updated by the FDA (https://www.fda.gov/media/134582/download) and EMA (https://www.ema.europa.eu/en/documents/scientific-guideline/guideline-investigation-drug-interactions_en.pdf).

Transporter biomarker research is drawing increasing attention from the pharmaceutical industry, academia, and regulatory authorities because biomarkers allows for early identification, prediction, and clinical monitoring of a specific drug interaction, reflecting the transporter inhibition liability of a drug candidate (Chu et al., 2017, Mariappan et al., 2017, Chu et al., 2018, Muller et al., 2018, Rodrigues et al., 2018, Shen, 2018). Plasma coproporphyrins I (CPI) and III

Downloaded from dmd.aspetjournals.org at ASPET Journals on April 18, 2024

DMD Fast Forward. Published on June 1, 2020 as DOI: 10.1124/dmd.120.090670
This article has not been copyedited and formatted. The final version may differ from this version.

(CPIII) were recently identified as novel endogenous biomarkers of hepatic OATP transporter function in monkeys and mice (Shen et al., 2016a). The oral administration of 100 mg/kg cyclosporin A (CsA) and 15 mg/kg rifampicin (RIF), two known OATP inhibitors, significantly increased the area under the plasma concentration-time curves (*AUC*s) of CPI and CPIII by 2.6- to 5.2-fold in monkeys (Shen et al., 2013, Shen et al., 2015). These changes are in agreement with those of rosuvastatin (RSV) in the same animals (2.6- to 5.2 fold vs. 2.9- to 6.3-fold). In addition, the plasma CPI and CPIII concentrations were markedly increased in Oatp1a/1b knockout mice compared to wild-type animals (7.1- to 18.4-fold), which were also in agreement with the increases in plasma RSV exposure (7.1- to 18.4-fold vs. 14.6-fold) (Shen et al., 2016a). Consequently, the clinical studies that assessed the dynamic changes and utility of plasma CP as an initial *in vivo* evaluation of weak to strong OATP1B1 and OATP1B3 inhibition were performed by different groups in the pharmaceutical industry and academia (Lai et al., 2016, Kunze et al., 2018a, Liu et al., 2018, Shen et al., 2018a, Takehara et al., 2018, Yee et al., 2019). The evaluation of CPI and CPIII as endogenous biomarkers of OATP1B inhibition in humans by quantitative scoring and prediction were demonstrated in those studies. CPI enabled *in vivo* assessment of inhibition potential of GDC-0810 towards OATP1B as early as Phase I ascending dose studies during drug development (Cheung et al., 2019). This novel biomarker is less expensive than a dedicated DDI study with a clinical probe and benefits downstream clinical plans by optimizing the development plan and prioritizing clinical studies (Chu et al., 2018, Muller et al., 2018, Shen et al., 2018b). Moreover, it is envisioned that CP will be utilized jointly with modeling tools to overcome current limitation of transporter *in vitro*-to-*in vivo* extrapolation (*IVIVE*) and greatly improve translational transporter-mediated DDI science (Wilson et al., 1988, Barnett et al., 2018, Yoshida et al., 2018, Yoshikado et al., 2018). To date, however, the pharmacokinetic characteristics including ADME

Downloaded from dmd.aspetjournals.org at ASPET Journals on April 18, 2024

DMD Fast Forward. Published on June 1, 2020 as DOI: 10.1124/dmd.120.090670
This article has not been copyedited and formatted. The final version may differ from this version.

of CPI and CPIII have not been studied. As endogenous substances that are subject to efficient biliary excretion, CPI and CPIII may also undergo enterohepatic recirculation. Therefore, understanding the oral absorption of CP is essentially important. In addition, there have not been reports of the *in vivo* selectivity of CP as a hepatic OATP1B transporter substrates when compared to major renal drug transporters including organic anion transporter (OAT) 1, OAT3, organic cation transporter (OCT) 2, multidrug and toxin extrusion protein (MATE) 1, and MATE2-K.

In recent years, the cynomolgus monkey has increasingly been utilized as an animal model to investigate clinical OATP1B-mediated inhibition by drugs such as RIF and CsA (Shen et al., 2013, Shen et al., 2015, Takahashi et al., 2016, Thakare et al., 2017b, De Bruyn et al., 2018, Ufuk et al., 2018, Takahashi et al., 2019, Zhang et al., 2019). As described herein, the absorption, distribution, and elimination of CPI were characterized by using deuterium- and tritium-labelled CPI in cynomolgus monkeys and 57BL6 mice, respectively. The first key question we wanted to address in this study was if deuterium labeled CPI would be extensively available after oral administration of octadeuterated coproporphyrin I (i.e., CPI-d8). The bioavailability of CPI in monkeys was determined by comparing the systemic exposures after a single intravenous (IV) dose of 0.1 mg/kg CPI-d8 and an oral (PO) dose of 0.2 mg/kg CPI-d8 in cynomolgus monkeys. Second, the volume of distribution at steady state, clearance, and elimination half-life were determined in monkeys after a single IV dose of 0.1 mg/kg CPI-d8. In addition, we were interested in investigating the extent of biodistribution of CP between blood, liver, kidney, and intestine by using quantitative whole-body autoradiography (QWBA) as this can differ and provide additional insights. Therefore, the tissue distribution was assessed in mice after a single IV dose of 0.04 mg/kg [^{3}H]CPI alone and with RIF (PO, 100 mg/kg) by QWBA. Lastly, for the sensitivity and selectivity of CP as an endogenous biomarker of hepatic OATP1B inhibition, an investigation was

Downloaded from dmd.aspetjournals.org at ASPET Journals on April 18, 2024

DMD Fast Forward. Published on June 1, 2020 as DOI: 10.1124/dmd.120.090670
This article has not been copyedited and formatted. The final version may differ from this version.

performed to analyze plasma CPI and CPIII concentrations in cynomolgus monkeys after single oral doses of CsA (4, 20, and 100 mg/kg). The highest dose of 100 mg/kg is selected because we previously reported that the systemic exposure after a single oral administration of 100 mg/kg CsA oral solution (Neoral) in cynomolgus monkeys was comparable to that at steady state after multiple doses in patients (Shen et al., 2013). In addition, animals also received a single IV dose of 0.1 mg/kg CPI-d8 to ensure that OATP1B was inhibited by CsA in a dose-dependent manner and allow comparison between endo- and exogenous probes. Moreover, an attempt was made to demonstrate CP as a selective biomarker for OATP1B inhibition by profiling CPI and CPIII in monkeys after single IV doses of probenecid (PROB), a potent inhibitor of organic anion transporter 1/3 (OAT1/3), or pyrimethamine (PYR), a potent inhibitor of organic cation transporter 2 (OCT2) and multidrug and toxin extrusion protein 1/2-K (MATE1/2-K).

Downloaded from dmd.aspetjournals.org at ASPET Journals on April 18, 2024

DMD Fast Forward. Published on June 1, 2020 as DOI: 10.1124/dmd.120.090670
This article has not been copyedited and formatted. The final version may differ from this version.

MATERIALS AND METHODS

Chemicals and Reagents. CPI-d8, CPIII-d8, and [^{3}H]CPI (4.9 Ci/mmol; >97.5% purity) were synthesized by Bristol-Myers Squibb (Princeton, NJ) (Supplemental Figures 1 A-C). CPI and CPIII were purchased from Frontier Scientific, Inc. (Logan, UT). Cyclosporine A (CsA), CsA-$^{13}C_2$, d4, rifampicin (RIF), probenecid (PROB), pyrimethamine (PYR), and CPI-$^{15}N_4$ were purchased from Toronto Research Chemicals (Toronto, ON, Canada). High-performance liquid chromatography (HPLC) grade methanol, acetonitrile, and water were obtained from Fisher Scientific (Fair Lawn, NJ). Formic acid and hydrochloric acid were obtained from EMD Chemicals Inc. (Gibbstown, NJ). CsA oral solution (Neoral, 100 mg/ml) was obtained from Novartis Pharmaceuticals (East Hanover, NJ). Cynomolgus monkey and human plasma that were stripped three times with charcoal were purchased from Bioreclamation IVT (Westbury, NY).

Pharmacokinetics Studies Employing Cynomolgus Monkeys and C57BL6 Mice. All animal experiments were performed at the Bristol Myers Squibb animal facility (Princeton, NJ) in accordance to the National Institutes of Health guidelines and were approved by the Bristol Myers Squibb Institutional Animal Care and Use Committee. Animals were housed in a temperature-controlled environment at 64 to 84 °F, 30 to 70% humidity, and a 12-hour (h) light-dark cycle.

Bioavailability of CPI-d8 and Effect of CsA Administration on Disposition of CPs in Monkeys. A crossover study design was used and the same three male cynomolgus monkeys (5.3 to 6.3 kg body weight) were dosed over a series of six treatments indicated in Table 1 with a 1-week washout between treatments.

Monkeys were fasted for 12 h before each oral dose but not the intravenous dose of CPI-d8 or CsA. Water was made available *ad libitum* and a daily ration of food was provided approximately 4 h post-dose during the study. CsA oral solution (Neoral) was given via oral

Downloaded from dmd.aspetjournals.org at ASPET Journals on April 18, 2024

DMD Fast Forward. Published on June 1, 2020 as DOI: 10.1124/dmd.120.090670
This article has not been copyedited and formatted. The final version may differ from this version.

gavage at 0 (blank vehicle), 4, 20, and 100 mg/kg (5 mL/kg) (Table 1). Sixty minutes (min) after the oral CsA administration, CPI-d8 was given by an oral administration at dose of 0.2 mg/kg [5 mL/kg; 5% DMSO and 95% water (v/v)] or an intravenous infusion via a femoral vein at dose of 0.1 mg/kg [1 mL/kg; 2% DMSO and 98% water (v/v)] over 10 min. Approximately 500 µL serial blood samples were collected in EDTA-anticoagulant via the cephalic or saphenous veins just before administration and at 0.17 (IV), 0.25, 0.5, 0.75, 1, 2, 3, 5, 7, and 24 h after CPI-d8 dosing. Fifty microliters of whole blood was aliquoted and transferred to tubes containing 450 µL of 50% methanol and 50% acetonitrile (v/v). The tubes were vortexed for a minimum of 20 seconds and the mixture were stored at ─70°C for CsA analysis. The remaining blood samples were centrifuged at 3,000g for 10 min at 2 to 8°C within 1 h of collection to generate plasma, and the samples were stored frozen at ─70°C until CPI-d8, CPI, and CPIII analysis. Urine was collected at intervals of 0–7 h and 7–24 h after administration of CPI-d8 using metabolism cages, and stored at ─70°C until analysis.

Effect of PROB and FSM Administration on Disposition of CPs in Monkeys. Plasma and urine samples were obtained from the pharmacokinetic interaction study between PROB and furosemide (FSM) in cynomolgus monkeys conducted previously (Shen et al., 2018c). Briefly, the samples were collected after intravenous administration of 2 mg/kg FSM alone, 40 mg/kg PROB alone, and coadministration of PROB or FSM, three-period crossover pharmacokinetic DDI study. In the third period, FSM was given to animals 30 min after PROB administration. Plasma samples before and 0.08, 0.17, 0.25, 0.5, 0.75, 1, 2, 3, 5, 7, and 24 h after the start of the FSM infusion were collected and stored at ─70°C until analysis.

Effect of PYR Administration on Disposition of CPs in Monkeys. Plasma and urine samples were obtained from the pharmacokinetic interaction study between PYR and metformin (MFM)

Downloaded from dmd.aspetjournals.org at ASPET Journals on April 18, 2024

DMD Fast Forward. Published on June 1, 2020 as DOI: 10.1124/dmd.120.090670
This article has not been copyedited and formatted. The final version may differ from this version.

in cynomolgus monkeys conducted previously (Shen et al., 2016b). Briefly, the samples were collected after intravenous administration of 3.9 mg/kg MFM alone and coadministration of PYR (0.5 mg/kg; IV) and MFM (3.9 mg/kg; IV). In the coadministration period, MFM was given to animals 60 min after PYR administration. Plasma samples before and 0.25, 0.5, 0.75, 1, 2, 3, 5, 7, 24, and 48 h after start of the MFM infusion were collected and stored at −70°C until analysis. However, the plasma CP levels were analyzed at 1, 5, and 24 h only due to availability of the plasma samples left from the original study. The mean concentrations of PYR at 1, 5, and 24 h postdose are 537, 567, and 174 nM, respectively (Shen et al., 2016b).

Effect of RIF Administration on Tissue Distribution of [^{3}H]CPI as Determined by QWBA in Mice. C57BL6 mice 8–10 week old weighing from 17 to 21 g were obtained from Charles River (Malvern, PA) and allowed to acclimate for at least 1 week before the start of the experiment. Eight mice were injected intravenously through the tail vein with 5 μL/g body weight at 8 μg/mL, to give a final dose of 0.04 mg/kg [^{3}H]CPI (5 mCi/kg) (n = 8). Additionally, 8 animals were injected with [^{3}H]CPI plus RIF (PO, 100 mg/kg), and a [^{3}H]CPI water solution was administered intravenously into mice 60 min after RIF administration. At the specified time after injection (2, 20 min, 3, or 24 h), two mice from each group were euthanized by CO_2 overexposure and were immediately frozen in a bath of hexane with dry ice. The biodistribution of [^{3}H]CPI was determined by QWBA as described below.

Frozen carcasses were embedded in chilled 2% of carboxymethylcellulose (Sakura Finetek, Torrance, CA). The embedded blocks were stored at −80°C until the time of sectioning to minimize diffusion of radiolabel materials into thawed tissues. Forty micrometer thick lengthwise whole-body sections were made by using a CM3600 (Leica microsystems, Nussloch, Germany). The sections used for autoradiography were left on the tape and placed on a [^{3}H]-

Downloaded from dmd.aspetjournals.org at ASPET Journals on April 18, 2024

DMD Fast Forward. Published on June 1, 2020 as DOI: 10.1124/dmd.120.090670
This article has not been copyedited and formatted. The final version may differ from this version.

sensitive phosphor imaging plate in a lead-shielded box at room temperature for three weeks. Afterwards, the plate was scanned in a Typhoon FLA 7000 image acquisition system (GE Healthcare Bio-Sciences, Pittsburgh, PA). The concentrations of total radiolabeled material in the tissues were determined by comparative densitometry and autoradiogram digital analysis as described previously (Shen et al., 2016c). Blood samples containing known amounts of radiolabeled compound treated under similar conditions were used as calibrators. Data for the concentration of [^{3}H]CPI in the animal tissues and organs were normalized by the whole body weight, in grams (i.e., the nCi [^{3}H]CPI/g).

Analytical Methods.

Liquid Chromatography-Tandem Mass Spectrometry (LC-MS/MS) Analysis of CsA in Blood. Blood concentrations of CsA were measured by LC-MS/MS as described previously, with some modifications (Shen et al., 2015). Briefly, a Shimazdzu ultraperformance liquid chromatography (UPLC) system (Shimadzu Corporation; Columbian, MD) was coupled to a Sciex API-6500 tandem mass spectrometer with a turbo-electrospray ionization source (Applied Biosystems, MDS Sciex; Toronto, Canada). Chromatographic separations were performed using an Acquity UPLC BEH C18 column (1.7 µm, 100 × 2.0 mm) (Waters Corporation, Milford, MA) maintained at 60°C. The mobile phase consisted of 0.1% formic acid in water (mobile phase A) and 0.1% formic acid in acetonitrile (mobile phase B), at a total flow rate of 0.7 mL/min. The gradient profile was held at 25% mobile phase B for 0.5 min, increased linearly to 100% in 2.5 min, held at 100% for 1.5 min, and finally brought back to 25% in 0.2 min followed by 1.3 min re-equilibration (total run time of 6 min per sample). Quantitative data were acquired in multiple reaction monitoring (MRM), and the transitions used were as follows: mass-to-charge ratio (m/z) 1219.5→m/z 1202.7 for CsA and m/z 1225.5→m/z 1207.7 for CsA-$^{13}C_2$, d4.

Downloaded from dmd.aspetjournals.org at ASPET Journals on April 18, 2024

DMD Fast Forward. Published on June 1, 2020 as DOI: 10.1124/dmd.120.090670
This article has not been copyedited and formatted. The final version may differ from this version.

Calibration curves were prepared in matrices by spiking 10 µL of appropriate standard solution at final concentrations ranging from 1 to 2,500 nM. For extraction of blood samples, 100 µL of acetonitrile containing 400 nM CsA-$^{13}C_2$, d4 as internal standard (IS) was added to 100 µL of blood sample mixture. Samples were then vortex-mixed for 5 min and the supernatants were transferred to a 0.45-µm multiscreen hydrophilic filtration plate (Millipore, MA). After centrifugation at room temperature, filtrate of each sample was collected in a 96-well plate. A 5-µL aliquot was injected for analysis by LC-MS/MS.

LC-MS/MS Analysis of CPI-d8, CPI, and CPIII in Plasma and Urine. The LC-MS/MS analysis of CPI-d8, CPI, and CPIII was performed as described previously, with some modifications (Lai et al., 2016, Kandoussi et al., 2018). Briefly, a Shimazdzu UPLC system (Shimadzu Corporation; Columbian, MD) was coupled to a Sciex API-6500 tandem mass spectrometer with a turbo-electrospray ionization source (Applied Biosystems, MDS Sciex; Toronto, Canada). The chromatographic separations were performed on a Waters Acquity UPLC BEH C18 column (1.7 µm, 100 × 2.0 mm) from Waters Corporation (Milford, MA) maintained at 65°C. The mobile phase consisted of 0.1% formic acid in water (A) and 0.1% formic acid in acetonitrile (B), which was delivered at a flow rate of 0.6 mL/min. The gradient profile was held at 28% mobile phase B for 0.5 min, increased linearly to 40% in 3.5 min, and then increased linearly to 95% in 0.5 min, held at 95% for 1 min, and finally brought back to 28% in 0.5 min followed by 1.0-min re-equilibration, resulting in total run time of 7 min per sample. Quantitative data were acquired in MRM-positive ionization mode. CP-d8, CP, and CPI-$^{15}N_4$ were detected at the selected reaction monitoring transitions of m/z 655.3→m/z 596.3, m/z 663.3→m/z 602.3, and m/z 659.3→m/z 600.3, respectively. Calibration curves were prepared in blank plasma and urine

Downloaded from dmd.aspetjournals.org at ASPET Journals on April 18, 2024

DMD Fast Forward. Published on June 1, 2020 as DOI: 10.1124/dmd.120.090670
This article has not been copyedited and formatted. The final version may differ from this version.

stripped with charcoal at concentrations ranging from 0.1-500 and 0.2-1,000 nM for CP and CP-d8, respectively.

The plasma and urine samples were extracted by using protein precipitation. Specifically, the 100 μL plasma and urine samples were mixed with 600 μL of ice-cold ethyl acetate containing 100 nM CPI-$^{15}N_4$ and 200 nM CPIII-d8 (internal standard), followed by vortex mixing on a mixer for 5 min at room temperature. The mixed solutions were then centrifuged at 4,000rpm for 15 min (Centrifuge model 5810R, Eppendorf), and the 400-μL supernatants were aspirated and evaporated. Samples were then reconstituted in 50 μL of 1 M formic acid solution. Five microliters of sample was injected for analysis.

Pharmacokinetic and Statistical Data Analysis. Phoenix WinNonlin® 8.1 software (CERTRA, Princeton, NJ) was used for analysis of pharmacokinetic parameters of CPI-d8, CsA, CPI and CPIII, following administration of probe with or without co-administration of transporter inhibitors. The area under the plasma concentration-time curve from zero to 24 h ($AUC_{0\text{-}24h}$) was calculated using mixed trapezoidal method while the area under the plasma concentration-time curve from zero to infinity (AUC_{tot}) includes $AUC_{0\text{-}24h}$ and that extrapolated from the last time point to infinity. The total plasma clearance (CL_{TOT}) was described by Equation 1:

$$CL_{\mathrm{TOT}} = \frac{Dose_{\mathrm{IV}}}{AUC_{\mathrm{TOT}}} \qquad \text{Equation 1}$$

The volume of distribution at steady-state (Vd_{SS}) was calculated by using the equation described as following:

$$Vd_{\mathrm{SS}} = \frac{Dose_{\mathrm{IV}} \times (AUMC)}{(AUC)^2} \qquad \text{Equation 2}$$

Downloaded from dmd.aspetjournals.org at ASPET Journals on April 18, 2024

DMD Fast Forward. Published on June 1, 2020 as DOI: 10.1124/dmd.120.090670
This article has not been copyedited and formatted. The final version may differ from this version.

where *AUMC* is the area under the curve of the first moment of the concentration-time curve. The Equation 3 was used to estimate the oral bioavailability (*F*):

$$F = \frac{Dose_{\mathrm{PO}} \times AUC_{\mathrm{IV}}}{Dose_{\mathrm{IV}} \times AUC_{\mathrm{PO}}} \qquad \text{Equation 3}$$

To analyze the statistically significant difference in the pharmacokinetic parameters of CPI-d8 between two sets of data in monkeys, a two-sided paired Student's *t* test was used because of the crossover design. One-way analysis of variance (ANOVA) was performed to assess CsA dose response by analyzing statistically significant differences in the pharmacokinetic parameters of CsA, CPI-d8, CPI, and CPIII among multiple CsA dose groups in monkeys. One-way ANOVA was also performed to evaluate the effect of PROB on CP systemic exposure by analyzing statistically significant differences in the pharmacokinetic parameters of CPI and CPIII among the administration of FSM alone, PROB alone, and PROB with FSM in monkeys. When a ratio showed that there were significant differences among CsA doses, the Dunnett method of multiple comparisons was used to determine which treatments differ. All statistical analyses were performed using Prism version 7.0 (GraphPad Software, Inc., San Diego, CA). A *p*-value of less than 0.05 was considered to be statistically significant (* $P < 0.05$, ** $P < 0.01$, and *** $P < 0.001$).

Downloaded from dmd.aspetjournals.org at ASPET Journals on April 18, 2024

DMD Fast Forward. Published on June 1, 2020 as DOI: 10.1124/dmd.120.090670
This article has not been copyedited and formatted. The final version may differ from this version.

RESULTS

Pharmacokinetics of CPI-d8 in Monkeys.

The mean plasma concentrations of CPI-d8, measured by LC/MS-MS, following a single dose of CPI-d8 alone or coadministration of CsA (PO, 100 mg/kg) in cynomolgus monkeys are summarized in Table 2, and the corresponding plasma concentration versus-time data are illustrated graphically in Figure 1. After IV administration of CPI-d8 alone, during the first 2-3 h after stopping the infusion, there was a rapid drop in plasma concentration followed by a slower elimination phase, exhibiting a multi-exponential decline (Figure 1). The CL_{TOT} of CPI-d8 was 10.1 ± 1.7 mL/min/kg. There is no report about the CPI blood to plasma partition. If there is no notable red blood cell partitioning, the blood clearance is low compared to monkey hepatic blood flow (i.e., 44 mL/min/kg) (Davies and Morris, 1993). The steady-state volume of distribution (Vd_{ss}) in monkeys was 0.57 L/kg (Table 2), indicating limited extravascular distribution. This Vd_{ss} is similar to total body water (i.e., 0.7 L/kg) (Davies and Morris, 1993). The $T_{1/2}$ was 7.6 ± 0.5 h. A single oral dose of 100 mg/kg CsA significantly increased the $AUC_{0\text{-}24h}$ (AUC_{TOT} of CPI-d8 (approximately 10-fold) ($p < 0.05$) compared with CPI-d8 alone (Figure 1 and Table 2). The apparent $T_{1/2}$ was significantly smaller in CPI-d8 alone than CsA treated groups (3.3 ± 1.1 vs. 7.6 ± 0.5 h; $p < 0.05$). A significant reduction in CL_{TOT} and Vd_{ss} of CPI-d8 was observed with CsA coadministration (1.3 ± 0.9 vs. 10.1 ± 1.7 mL/min/kg and 0.24 ± 0.13 vs. 0.57 ± 0.10 L/kg, respectively) ($p < 0.01$) (Table 2).

After oral administration of CPI-d8 alone, CPI-d8 was rapidly absorbed (T_{max} = 1.5 ± 1.3 h), with a bioavailability of 3.2 ± 1.7 % (Figure 1 and Table 2). The maximum plasma concentration (C_{max}) and $AUC_{0\text{-}24h}$ of CPI-d8 in plasma were 1.1 ± 0.5 nM and 9.8 ± 3.0 nM•h, respectively. Likewise, the coadministration of CsA increased CPI-d8 systemic exposure after oral

Downloaded from dmd.aspetjournals.org at ASPET Journals on April 18, 2024

DMD Fast Forward. Published on June 1, 2020 as DOI: 10.1124/dmd.120.090670
This article has not been copyedited and formatted. The final version may differ from this version.

CPI-d8 dosing, although with lower fold changes of $AUC_{0\text{-}24h}$ and AUC_{TOT} (2.8- and 2.4-fold, respectively), compared with IV administration (Figure 1 and Table 2). Marked increases in CPI-d8 C_{max} were also observed after CsA administration, with fold change of approximately 2.2-fold ($p > 0.05$) (Figure 1 and Table 2). CsA administration may decrease CPI-d8 oral bioavailability versus the control, with bioavailability values of 0.8 ± 0.6 and 3.2 ± 1.7 %, respectively (Figure 1 and Table 2). However, the difference is not statistically significant ($p > 0.05$). The large interindividual variability potentially affected the statistical assessment.

Pharmacokinetics of CsA in Monkeys.

The mean CsA blood concentration versus time profiles following the administration of a single oral dose of 4, 20, and 100 mg/kg CsA to male cynomolgus monkeys are illustrated in Figure 2. Increase in blood Cmax after a single dose of CsA was nearly proportional to the dose increment between 4 and 100 mg/kg doses (0.19 ± 0.04 and 3.8 ± 2.3 μM, respectively), and it was more proportional to the dose increment between 4 and 20 mg/kg (0.19 ± 0.04 and 2.5 ± 1.6 μM, respectively) (Table 3). In contrast, following a single oral administration of 4 to 100 mg/kg CsA, the increase in blood $AUC_{0\text{-}24h}$ was less proportional to the dose increment between 4 and 100 mg/kg (2.7 ± 0.6 and 26.6 ± 4.1 μM●h, respectively) whereas approximately proportional to the dose increment between 4 and 20 mg/kg (2.7 ± 0.6 and 10.5 ± 7.5 μM●h, respectively) (Table 3). The oral exposure of CsA at 20 mg/kg was comparable to those reported in cynomolgus monkeys previously (Schuurman et al., 2001, Shen et al., 2015).

Effects of CsA Administration on Plasma CP Levels.

Figure 3 shows the means ± SD of plasma concentrations of exogenous and endogenous CP versus-time for the entire study period, which includes vehicle, 4, 20, and 100 mg/kg CsA administration periods. Table 4 summarizes the exposures during the 4 periods. Compared with

Downloaded from dmd.aspetjournals.org at ASPET Journals on April 18, 2024

DMD Fast Forward. Published on June 1, 2020 as DOI: 10.1124/dmd.120.090670
This article has not been copyedited and formatted. The final version may differ from this version.

the vehicle control, CPI-d8 $AUC_{0\text{-}24h}$ was significantly increased 1.8 ± 0.3-, 6.2 ± 2.5-, and 10.5 ± 6.8-fold by 4, 20, and 100 mg/kg CsA, respectively ($p < 0.05$). At all CsA dose levels, the recovery of unchanged CPI-d8 in urine was less than expected. The urinary recovery at 100 mg/kg CsA was only approximately 40% of the dose. The poor recovery is likely due to the destruction and loss of CP by light during the urine collection using metabolic cages. As a result, the pharmacokinetic analysis of CPI-d8, CPI, and CPIII in urine was not performed. In contrast, plasma was prepared within 30 min of blood collection and stored in a freezer which was protected from light. The plasma concentrations of CP in this study were similar to those reported previously.

As with CPI-d8, the plasma levels of endogenous CPI and CPIII were measured in cynomolgus monkeys after increasing doses of CsA. In agreement, CPI and CPIII exhibited a marked dose-dependent increase in their plasma concentration-time profile (Figures 3B and 3C; Table 4). Compared with the vehicle control, the $AUC_{0\text{-}24h}$ and C_{max} of CPI and CPIII were increased 1.1- to 1.6-. 1.4- to 3.8-, and 4.5- to 6.9-fold at 4, 20, and 100 mg/kg CsA, respectively, although the increases were generally less proportional to the CsA dose increment (Figure 5). In addition, the increase was only statistically significant at 20 and 100 mg/kg CsA (Table 4).

Correlation between Increased Plasma Concentrations of Exogenous and Endogenous CP by CsA.

To further study the potential of plasma concentrations of CPI and CPIII as an endogenous biomarker of OATP1B activity, the fold change in CP $AUC_{0\text{-}24h}$ (*AUCR*) was correlated with that of CPI-d8 after increasing doses of CsA in this study. A good linear correlation ($R^2 = 0.920$) between CPI *AUCR* and CPIII *AUCR* was observed (Figure 4A), indicating comparable CsA dose response between endogenous plasma CPI and CPIII concentrations. More importantly, Figures 4B and 4C showed the presence of a significant and positive correlation using linear regression

Downloaded from dmd.aspetjournals.org at ASPET Journals on April 18, 2024

DMD Fast Forward. Published on June 1, 2020 as DOI: 10.1124/dmd.120.090670
This article has not been copyedited and formatted. The final version may differ from this version.

between CPI and CPI-d8 *AUCR*, and CPIII and CPI-d8 *AUCR*, respectively (R^2 of 0.680 and 0.718, respectively; $p < 0.001$).

To assess CsA dose response, an effort was made to correlate CP *AUCR* with CsA C_{max} , $AUC_{0\text{-}24h}$, and maximum unbound hepatic inlet concentration ($I_{in,max,u}$) that varied over a wide range in this study (Figure 5 and Table 5). A modest linear correlation between CsA C_{max} or $AUC_{0\text{-}24h}$ and CP *AUCR* was observed (R^2 of 0.523 and 0.447, respectively; $p < 0.05$). The results of in vitro-to-in vivo extrapolation analysis of DDI magnitude using a mechanistic static model are summarized in Table 5. The magnitude of the area under the plasma concentration-time curve ratios (*AUCR*s) in the presence of 4, 20 and 100 mg/kg CsA are predicted to be 1.58, 4.06 and 15.4, respectively, using the cynomolgus monkey OATP1B1 IC_{50} value of 0.28 μM determined previously (Shen et al., 2013) (Table 5). Similarly, the *AUCR*s are 1.65, 4.42, and 17.1, respectively, using the reported CsA monkey OATP1B3 IC_{50} of 0.25 μM (Shen et al., 2013). The predicted *AUCR* values were within 1.6-fold of the observed data for CPI-d8 whereas the approach substantially overpredicted the observed *AUCR* of CPI and CPIII (1.5- to 3.9-fold), highlighting the difference of DDI magnitude between exogenous and endogenous coproporphyrins. This is likely due to altered efflux of endogenous coproporphyrins from the hepatocytes and erythrocytes, the biosynthesis sites of CPI and CPIII, in the presence of CsA, which was not the case for exogenous CPI-d8.

Effects of PROB Administration on Plasma CP Levels.

The systemic exposures of CPI and CPIII were determined after an IV dose of 2 mg/kg FSM alone, 40 mg/kg PROB alone, or PROB plus FSM in cynomolgus monkeys (Table 6, Supplemental Figure 2). Compared with the FSM group, CPI $AUC_{0\text{-}24h}$ and C_{max} were decreased 11% to 25% with PROB treatment either alone or coadministered with FSM ($p > 0.05$) (Table 6).

Downloaded from dmd.aspetjournals.org at ASPET Journals on April 18, 2024

DMD Fast Forward. Published on June 1, 2020 as DOI: 10.1124/dmd.120.090670
This article has not been copyedited and formatted. The final version may differ from this version.

Furthermore, CPIII $AUC_{0\text{-}24h}$ and C_{max} were increased 1.5 ± 0.4 - to 2.5 ± 0.8-fold by PROB; however, the change was not statistically significant (Table 6).

Effects of PYR Administration on Plasma CP Levels.

Figure 6 illustrates the mean ± SD of plasma concentrations of CPI and CPIII at 1, 5, and 24 h after a single IV dose of 3.9 mg/kg MFM alone or MFM plus PYR (IV, 0.5 mg/kg). Plasma CP concentrations were comparable and not statistically different between MFM alone and PYR plus MFM periods, indicating no major effect of PYR on CP.

Biodistribution of [^{3}H]CPI in Mice.

The QWBA images and tissue concentrations of [^{3}H]CPI at 2 and 20 min, 3, and 24 h after IV injection into normal C57BL6 wild type mice is shown in Supplemental Figure 3 and Table 7. As expected, the liver, kidney and intestine were the major sites of distribution of [^{3}H]CPI (Table 7 and Supplement Figures 3A and 3B). High levels were also found in the blood. These high activities are consistent with the known elimination routes of CPI (Shen et al., 2016a). High levels of radioactivity in the lung may be associated with [^{3}H]CPI in the blood in this highly perfused tissue and [^{3}H]CPI clears from the lung with a half-life similar to the plasma half-life (Table 7). The brain had relatively low radioactivity.

The radioactivity in blood after intravenous administration of [^{3}H]CPI in control and RIF-treated mice decayed rapidly (Table 7). However, the blood terminal $T_{1/2}$ of [^{3}H]CPI appeared to be affected by RIF, as the blood concentration of [^{3}H]CPI at 20 min were markedly increased in the presence of RIF (300 vs. 110 nCi/g). Consistently, RIF noticeably increased the distribution of [^{3}H]CPI radioactivity in the kidney (*AUC*: 681 vs. 154 nCi●h/g) whereas it had less pronounced impact within the liver (*AUC*: 804 vs. 557 nCi●h/g).

Downloaded from dmd.aspetjournals.org at ASPET Journals on April 18, 2024

DMD Fast Forward. Published on June 1, 2020 as DOI: 10.1124/dmd.120.090670
This article has not been copyedited and formatted. The final version may differ from this version.

DISCUSSION

The recent growing interest in the use of coproporphyrins as endogenous biomarkers of OATP1B activity has resulted in questions about its ADME properties. Another related, albeit unproven concern, is the enterohepatic circulation of CPs, which may also hypothetically preclude achieving an optimal prediction of OATP1B activity by using CPs. Furthermore, the in vivo sensitivity and selectivity of CPs as biomarkers of OATP1B have not been fully investigated. For these reasons, noncommercially available deuterium- and tritium-labeled CPI (CPI-d8 and [^{3}H]CPI) were prepared, and the pharmacokinetics and biodistribution of CPI-d8 and [^{3}H]CPI were profiled in cynomolgus monkeys and C57BL6 mice, respectively. Furthermore, the plasma CPs at different doses of CsA, an OATP1B inhibitor, were characterized in monkeys. We also evaluate the effects of the inhibitors of organic anion transporters (PROB) and organic cation transporters (PYR) on plasma CP levels in monkeys.

We employed cynomolgus monkeys for CPI pharmacokinetics and drug interaction analysis because the cynomolgus monkey model was recently used to examine OATP1B-mediated DDI and predict human in vivo intrinsic hepatic clearance from cynomolgus monkey and human hepatocyte uptake for OATP substrates (Shen et al., 2013, Takahashi et al., 2013, Chu et al., 2015, Thakare et al., 2017a, De Bruyn et al., 2018, Ufuk et al., 2018). This is particularly important because the OATP1B amino acid sequence and transport activity are known to be highly similar between cynomolgus monkeys and humans (Shen et al., 2013). CPI-d8 displayed moderate $T_{1/2}$ and Vd_{ss} in cynomolgus monkeys (7.6 ± 0.5 h and 0.57 ± 0.10 L/kg, respectively) (Figure 1 and Table 2). The $T_{1/2}$ is appropriate for an endogenous biomarker of drug metabolizing enzymes or transporters. For example, the rate of elimination of 4β-hydroxycholesterol, an endogenous marker

Downloaded from dmd.aspetjournals.org at ASPET Journals on April 18, 2024

DMD Fast Forward. Published on June 1, 2020 as DOI: 10.1124/dmd.120.090670
This article has not been copyedited and formatted. The final version may differ from this version.

of CYP3A4/5 activity in humans, is slow ($T_{1/2}$ 17 days), which limits its use to study rapid changes in CYP3A activity. In addition, we report for the first time that the absolute bioavailability of oral CPI (0.2 mg/kg CPI-d8) is averaged 3.2 ± 1.7%. CsA (PO, 100 mg/kg), a pan-inhibitor of intestinal P-gp and BCRP, and hepatic OATP, had no significant effect on the oral absorption and bioavailability of CPI-d8 compared to the vehicle control although the mean bioavailability was decreased by CsA (0.8 ± 0.6% vs. 3.2 ± 1.7%) ($p > 0.05$) (Table 2). These results are consistent with the in vitro human transporter phenotyping data. The studies from transporter transfected systems showed CPI was not a substrate for human intestinal transporters including P-gp, BCRP, or OATP2B1 although the substrate potential of CPI towards transporters may display a difference between cynomolgus monkeys and humans (Bednarczyk and Boiselle, 2016, Shen et al., 2017, Kunze et al., 2018a). It is worth noting that the enterohepatic circulation of CPI was reported in a clinical study performed several decades ago (Koskelo and Kekki, 1976). In these early studies, enterohepatic circulation was usually concluded by observation of a ‘‘secondary peak’’ in the time vs. concentration curve after a single intravenous administration, but pertinent mechanism(s) explaining the secondary peak were not rigorously investigated. In fact, except for the report several decades ago, the enterohepatic circulation of CPI has not been reported. In addition, Takehara et al. (2019) have recently shown via bile duct cannulation data that CPI and CPIII did not undergo enterohepatic circulation in cynomolgus monkeys (Takehara et al., 2019). Plasma CPI and CPIII concentrations were not altered in bile duct-cannulated monkeys compared to normal animals (Takehara et al., 2019). In contrast, bile flow diversion markedly decreased the plasma level of bile acid-O-sulfates such as glycochenodeoxycholic acid 3-O-sulfate (GCDCA-S). The intestinal absorption of bile acids but not coproporphyrins plays an important role in their

Downloaded from dmd.aspetjournals.org at ASPET Journals on April 18, 2024

DMD Fast Forward. Published on June 1, 2020 as DOI: 10.1124/dmd.120.090670
This article has not been copyedited and formatted. The final version may differ from this version.

homeostasis (Takehara et al., 2019). Taken together, CPI does not undergo enterohepatic circulation in cynomolgus monkeys.

The mouse study shows the rapid and selective elimination of radiolabeled CPI via the liver and kidney. After intravenous injection of [^{3}H]CPI in mice, the liver, kidney, and intestinal tissues, had relatively high uptake and exposure, demonstrating the specificity of CPI for these elimination organs (Supplemental Figure 3A and Table 7). The uptake in the lung at 2 min was comparable to that in the liver but then declined in parallel to the blood concentration, suggesting that lung exposure was due to the high blood volume in this tissue. Other tissues such as brain and muscle had relatively low values for [^{3}H]CPI concentration. The biodistribution of CPI in mice in the presence of RIF, a hepatic OATP inhibitor, differs considerably from that in the absence of the inhibitor (Supplemental Figure 3 and Table 7). The maximal distribution of [^{3}H]CPI to the intestine was 1350 nCi [^{3}H]CPI/g (at 3 h) in the coadministration group whereas [^{3}H]CPI was rapidly eliminated to the intestine in the absence of RIF (maximal distribution of 5850 nCi [^{3}H]CPI/g at 20 min). In addition, the uptake of [^{3}H]CPI into the liver was inhibited by RIF (maximal uptake of 360 versus 150 nCi [^{3}H]CPI/g). In contrast, the distribution of [^{3}H]CPI radioactivity in the kidney was increased by RIF (*AUC*: 681 vs. 154 nCi●h/g). These results are consistent with the pattern of CPI excretion in rodent (Kaplowitz et al., 1972) and human bile and urine (Aziz and Watson, 1969, Mustajoki and Koskelo, 1976, Rocchi et al., 1984). It has been demonstrated that approximately 70% to 80% of the daily CPI is found in the bile whereas the remainder is excreted in the urine of healthy subjects. With impairment of hepatic excretory function by genetic mutation (i.e., Rotor syndrome) or chemical inhibitors (such as oral contraceptive agents, RIF, and CsA), there is an increase in the CPI excreted in urine (Koskelo et al., 1966, Ben-Ezzer et al., 1971, Wolkoff et al., 1976, Shimizu et al., 1981, Lai et al., 2016, Shen et al., 2018b, Yee et al., 2019).

Downloaded from dmd.aspetjournals.org at ASPET Journals on April 18, 2024

DMD Fast Forward. Published on June 1, 2020 as DOI: 10.1124/dmd.120.090670
This article has not been copyedited and formatted. The final version may differ from this version.

This change in the pattern of CPI excretion is consistent with the observation of [^{3}H]CPI in the mice pretreated with RIF in this study (Supplemental Figure 3 and Table 7). Of note, the recovery of unchanged CPI-d8 in urine was less than expected in cynomolgus monkeys. The urinary recovery following IV administration of 0.1 mg/kg CPI-d8 alone and in combination with 100 mg/kg CsA were 4.2% and 40% of the dose, respectively. The poor recovery may be due to the destruction of CP by light during the urine collection using metabolic cages. In contrast, plasma was prepared within 30 min of blood collection and stored in a freezer, protected from light. The plasma levels of CPI and CPIII are similar to those reported before.

To assess the CsA dose-dependent response, CsA Neoral microemulsion was administered to cynomolgus monkeys at three dose levels of 4, 20, and 100 mg/kg along with CPI-d8. As shown in Figure 2A and Table 3, mean total blood C_{max} values of 0.19, 2.5, and 3.8 μM and $AUC_{0\text{-}24h}$ values of 2.7, 10.5, and 26.6 μM●h were found at 4, 20, and 100 mg/kg CsA, respectively. These pharmacokinetic parameters are similar to the nonhuman primate data reported previously (Schuurman et al., 2001, Shen et al., 2015). Apparently, the increases in C_{max} and $AUC_{0\text{-}24h}$ were generally proportional to dose between 4 and 20 mg/kg while those were less than dose proportional between 20 and 100 mg/kg (Figures 2B and 2C). Despite the nonlinearity, there was a modest linear correlation between CsA blood C_{max} or $AUC_{0\text{-}24h}$ and CP *AUCR* (R^2 of 0.523 and 0.447, respectively; $p < 0.05$) (Figure 5). A clear CsA dose-dependent increase in the *AUCR*s of CPI-d8 (1.8, 6.2, and 10.5), CPI (1.1, 1.4, and 4.4), and CPIII (1.1, 1.8, and 4.6) were observed (Table 4). These CsA dose response results indicate that CPI and CPIII are sensitive OATP1B endogenous biomarkers. However, the magnitude of the *AUCR*s of CPI-d8 in the presence of 4, 20, and 100 mg/kg CsA are greater than those of CPI and CPIII (Table 5). This is likely due to the reduced efflux of endogenous CPs but not exogenous CPI-d8 from the hepatocytes and

Downloaded from dmd.aspetjournals.org at ASPET Journals on April 18, 2024

DMD Fast Forward. Published on June 1, 2020 as DOI: 10.1124/dmd.120.090670
This article has not been copyedited and formatted. The final version may differ from this version.

erythrocytes. It has been reported that CPI and CPIII are substrates of MRP3 (Kunze et al., 2018b). BMS studies also show that both CPI and CPIII are substrate of MRP4 (unpublished data).

To further study the selectivity of CPs as probes of OATP1B over OAT1, OAT3, OCT2, MATE1, and MATE2-K, we evaluated the effects of a renal organic anion transporter inhibitor PROB (IV, 40 mg/kg) and an organic cation transporter inhibitor PYR (IV, 0.5 mg/kg) on plasma CP levels in cynomolgus monkeys (Figure 6 and Supplemental Figures 2). The plasma samples were obtained from our previous study, in which PROB increased the area under the *AUC* of coadministered furosemide, a known substrate of OAT1 and OAT3, by 4.1-fold in same animals (Shen et al., 2018c). There were generally no statistically significant increases in plasma concentrations of CPI or CPIII observed even though mean CPIII exhibited increased $AUC_{0\text{-}24h}$ and C_{max} ratio by PROB (1.5- to 2.5-fold) (Table 6). This may be attributed to large inter-individual variability in plasma CPIII levels in cynomolgus monkeys. In addition, it has been reported that oral administration of 30 mg/kg PROB increased plasma pitavastatin and rosuvastatin exposures by approximately 2- to 3-fold in cynomolgus monkeys through OATP1B inhibition (Kosa et al., 2018). Consistently, PROB significantly inhibited the uptake of pitavastatin and rosuvastatin in monkey hepatocytes (Kosa et al., 2018). When studying effect of PYR on CP exposure at the IV dose of 0.5 mg/kg in cynomolgus monkeys, no statistically significant increases in plasma concentrations and urinary excretion rate of CPI and CPIII were observed (Figure 6). In contrast, our previous study showed that the intravenous pretreatment of the same animals with 0.5 mg/kg PYR increased the *AUC* by 2.2-fold compared to vehicle control (Shen et al., 2016b).

In conclusion, following a series of in vivo cynomolgus monkey and mouse studies, we demonstrated that CPI displayed limited oral absorption, a short half-life, and low exposure to

Downloaded from dmd.aspetjournals.org at ASPET Journals on April 18, 2024

DMD Fast Forward. Published on June 1, 2020 as DOI: 10.1124/dmd.120.090670
This article has not been copyedited and formatted. The final version may differ from this version.

tissues except for elimination organs. We also established that CPI and CPIII in plasma are sensitive and selective biomarkers reflecting OATP1B inhibition over OAT1/3 and OCT2-/MATE1/2-K inhibition in monkeys. Moreover, we have shown that OATP1B inhibition can alter the biodistribution and elimination of CPI. These results suggest that hepatic OATP transporters are major determinants of the disposition of CPI in cynomolgus monkeys and mice and CPI is a sensitive and selective endogenous biomarker of hepatic OATP inhibition.

Downloaded from dmd.aspetjournals.org at ASPET Journals on April 18, 2024

DMD Fast Forward. Published on June 1, 2020 as DOI: 10.1124/dmd.120.090670
This article has not been copyedited and formatted. The final version may differ from this version.

Authorship Contributions

Participated in research design: Jinping Gan, Yang Hong, Yurong Lai, Michael Sinz, and Hong Shen,

Conducted experiments: Xiaomei Gu, Lifei Wang, and Yuan Tian

Contributed new reagents or analytic tools: Xiaomei and Hong Shen

Performed data analysis: Xiaomei Gu, Lifei Wang, Jinping Gan, Yurong Lai, and Hong Shen

Wrote or contributed to the writing of the manuscript: Xiaomei Gu, Lifei Wang, Jinping Gan Yurong Lai, Michael Sinz, and Hong Shen

Downloaded from dmd.aspetjournals.org at ASPET Journals on April 18, 2024

DMD Fast Forward. Published on June 1, 2020 as DOI: 10.1124/dmd.120.090670
This article has not been copyedited and formatted. The final version may differ from this version.

References

Awni WM, Kasiske BL, Heim-Duthoy K and Rao KV (1989) Long-term cyclosporine pharmacokinetic changes in renal transplant recipients: effects of binding and metabolism. *Clin Pharmacol Ther* 45: 41-48.

Aziz MA and Watson CJ (1969) An analysis of the porphyrins of normal and cirrhotic human liver and normal bile. *Clin Chim Acta* 26: 525-531.

Barnett S, Ogungbenro K, Menochet K, Shen H, Lai Y, Humphreys WG and Galetin A (2018) Gaining Mechanistic Insight Into Coproporphyrin I as Endogenous Biomarker for OATP1B-Mediated Drug-Drug Interactions Using Population Pharmacokinetic Modeling and Simulation. *Clin Pharmacol Ther* 104: 564-574.

Bednarczyk D and Boiselle C (2016) Organic anion transporting polypeptide (OATP)-mediated transport of coproporphyrins I and III. *Xenobiotica* 46: 457-466.

Ben-Ezzer J, Rimington C, Shani M, Seligsohn U, Sheba C and Szeinberg A (1971) Abnormal excretion of the isomers of urinary coproporphyrin by patients with Dubin-Johnson syndrome in Israel. *Clin Sci* 40: 17-30.

Cheung KWK, Yoshida K, Cheeti S, Chen B, Morley R, Chan IT, Sahasranaman S and Liu L (2019) GDC-0810 Pharmacokinetics and Transporter-Mediated Drug Interaction Evaluation with an Endogenous Biomarker in the First-in-Human, Dose Escalation Study. *Drug Metab Dispos* 47: 966-973.

Chu X, Chan GH and Evers R (2017) Identification of Endogenous Biomarkers to Predict the Propensity of Drug Candidates to Cause Hepatic or Renal Transporter-Mediated Drug-Drug Interactions. *J Pharm Sci* 106: 2357-2367.

Chu X, Liao M, Shen H, Yoshida K, Zur AA, Arya V, Galetin A, Giacomini KM, Hanna I, Kusuhara H, Lai Y, Rodrigues D, Sugiyama Y, Zamek-Gliszczynski MJ, Zhang L and International Transporter C (2018) Clinical Probes and Endogenous Biomarkers as Substrates for Transporter Drug-Drug Interaction Evaluation: Perspectives From the International Transporter Consortium. *Clin Pharmacol Ther* 104: 836-864.

Chu X, Shih SJ, Shaw R, Hentze H, Chan GH, Owens K, Wang S, Cai X, Newton D, Castro-Perez J, Salituro G, Palamanda J, Fernandis A, Ng CK, Liaw A, Savage MJ and Evers R (2015) Evaluation of cynomolgus monkeys for the identification of endogenous biomarkers

Downloaded from dmd.aspetjournals.org at ASPET Journals on April 18, 2024

DMD Fast Forward. Published on June 1, 2020 as DOI: 10.1124/dmd.120.090670
This article has not been copyedited and formatted. The final version may differ from this version.

for hepatic transporter inhibition and as a translatable model to predict pharmacokinetic interactions with statins in humans. *Drug Metab Dispos* 43: 851-863.

Davies B and Morris T (1993) Physiological parameters in laboratory animals and humans. *Pharm Res* 10: 1093-1095.

De Bruyn T, Ufuk A, Cantrill C, Kosa RE, Bi YA, Niosi M, Modi S, Rodrigues AD, Tremaine LM, Varma MVS, Galetin A and Houston JB (2018) Predicting Human Clearance of Organic Anion Transporting Polypeptide Substrates Using Cynomolgus Monkey: In Vitro-In Vivo Scaling of Hepatic Uptake Clearance. *Drug Metab Dispos* 46: 989-1000.

Drewe J, Beglinger C and Kissel T (1992) The absorption site of cyclosporin in the human gastrointestinal tract. *Br J Clin Pharmacol* 33: 39-43.

Group SC, Link E, Parish S, Armitage J, Bowman L, Heath S, Matsuda F, Gut I, Lathrop M and Collins R (2008) SLCO1B1 variants and statin-induced myopathy--a genomewide study. *N Engl J Med* 359: 789-799.

Kandoussi H, Zeng J, Shah K, Paterson P, Santockyte R, Kadiyala P, Shen H, Shipkova P, Langish R, Burrrell R, Easter J, Mariannino T, Marathe P, Lai Y, Zhang Y and Pillutla R (2018) UHPLC-MS/MS bioanalysis of human plasma coproporphyrins as potential biomarkers for organic anion-transporting polypeptide-mediated drug interactions. *Bioanalysis* 10: 633-644.

Kaplowitz N, Javitt N and Kappas A (1972) Coproporphyrin I and 3 excretion in bile and urine. *J Clin Invest* 51: 2895-2899.

Konig J, Seithel A, Gradhand U and Fromm MF (2006) Pharmacogenomics of human OATP transporters. *Naunyn Schmiedebergs Arch Pharmacol* 372: 432-443.

Kosa RE, Lazzaro S, Bi YA, Tierney B, Gates D, Modi S, Costales C, Rodrigues AD, Tremaine LM and Varma MV (2018) Simultaneous Assessment of Transporter-Mediated Drug-Drug Interactions Using a Probe Drug Cocktail in Cynomolgus Monkey. *Drug Metab Dispos* 46: 1179-1189.

Koskelo P, Eisalo A and Toivonen I (1966) Urinary excretion of porphyrin precursors and coproporphyrin in healthy females on oral contraceptives. *Br Med J* 1: 652-654.

Koskelo P and Kekki M (1976) Multicompartment analysis of 14C-labelled coproporphyrin and uroporphyrin kinetics in human beings. *Ann Clin Res* 8 Suppl 17: 198-202.

Downloaded from dmd.aspetjournals.org at ASPET Journals on April 18, 2024

DMD Fast Forward. Published on June 1, 2020 as DOI: 10.1124/dmd.120.090670
This article has not been copyedited and formatted. The final version may differ from this version.

Kunze A, Ediage EN, Dillen L, Monshouwer M and Snoeys J (2018a) Clinical Investigation of Coproporphyrins as Sensitive Biomarkers to Predict Mild to Strong OATP1B-Mediated Drug-Drug Interactions. *Clin Pharmacokinet* 57: 1559-1570.

Kunze A, Ediage EN, Dillen L, Monshouwer M and Snoeys J (2018b) Clinical Investigation of Coproporphyrins as Sensitive Biomarkers to Predict Mild to Strong OATP1B-Mediated Drug-Drug Interactions. *Clin Pharmacokinet*.

Lai Y, Mandlekar S, Shen H, Holenarsipur VK, Langish R, Rajanna P, Murugesan S, Gaud N, Selvam S, Date O, Cheng Y, Shipkova P, Dai J, Humphreys WG and Marathe P (2016) Coproporphyrins in Plasma and Urine Can Be Appropriate Clinical Biomarkers to Recapitulate Drug-Drug Interactions Mediated by Organic Anion Transporting Polypeptide Inhibition. *J Pharmacol Exp Ther* 358: 397-404.

Liu L, Cheeti S, Yoshida K, Choo E, Chen E, Chen B, Gates M, Singel S, Morley R, Ware J and Sahasranaman S (2018) Effect of OATP1B1/1B3 Inhibitor GDC-0810 on the Pharmacokinetics of Pravastatin and Coproporphyrin I/III in Healthy Female Subjects. *J Clin Pharmacol* 58: 1427-1435.

Mariappan TT, Shen H and Marathe P (2017) Endogenous Biomarkers to Assess Drug-Drug Interactions by Drug Transporters and Enzymes. *Curr Drug Metab* 18: 757-768.

Marzolini C, Tirona RG and Kim RB (2004) Pharmacogenomics of the OATP and OAT families. *Pharmacogenomics* 5: 273-282.

Mueller EA, Kovarik JM, van Bree JB, Tetzloff W, Grevel J and Kutz K (1994) Improved dose linearity of cyclosporine pharmacokinetics from a microemulsion formulation. *Pharm Res* 11: 301-304.

Muller F, Sharma A, Konig J and Fromm MF (2018) Biomarkers for In Vivo Assessment of Transporter Function. *Pharmacol Rev* 70: 246-277.

Mustajoki P and Koskelo P (1976) Hereditary hepatic porphyrias in Finland. *Acta Med Scand* 200: 171-178.

Rocchi E, Balli F, Gibertini P, Trenti T, Pietrangelo A, Cassanelli M, Frigieri G and Ventura E (1984) Coproporphyrin excretion in healthy newborn babies. *J Pediatr Gastroenterol Nutr* 3: 402-407.

Rodrigues AD, Taskar KS, Kusuhara H and Sugiyama Y (2018) Endogenous Probes for Drug Transporters: Balancing Vision With Reality. *Clin Pharmacol Ther* 103: 434-448.

Downloaded from dmd.aspetjournals.org at ASPET Journals on April 18, 2024

DMD Fast Forward. Published on June 1, 2020 as DOI: 10.1124/dmd.120.090670
This article has not been copyedited and formatted. The final version may differ from this version.

Schuurman HJ, Slingerland W, Mennninger K, Ossevoort M, Hengy JC, Dorobek B, Vonderscher J, Ringers J, Odeh M and Jonker M (2001) Pharmacokinetics of cyclosporine in monkeys after oral and intramuscular administration: relation to efficacy in kidney allografting. *Transpl Int* 14: 320-328.

Shen H (2018) A pharmaceutical industry perspective on transporter and CYP-mediated drug-drug interactions: kidney transporter biomarkers. *Bioanalysis* 10: 625-631.

Shen H, Chen W, Drexler DM, Mandlekar S, Holenarsipur VK, Shields EE, Langish R, Sidik K, Gan J, Humphreys WG, Marathe P and Lai Y (2017) Comparative Evaluation of Plasma Bile Acids, Dehydroepiandrosterone Sulfate, Hexadecanedioate, and Tetradecanedioate with Coproporphyrins I and III as Markers of OATP Inhibition in Healthy Subjects. *Drug Metab Dispos* 45: 908-919.

Shen H, Christopher L, Lai Y, Gong J, Kandoussi H, Garonzik S, Perera V, Garimella T and Humphreys WG (2018a) Further Studies to Support the Use of Coproporphyrin I and III as Novel Clinical Biomarkers for Evaluating the Potential for Organic Anion Transporting Polypeptide 1B1 and OATP1B3 Inhibition. *Drug Metab Dispos* 46: 1075-1082.

Shen H, Christopher L, Lai Y, Gong J, Kandoussi H, Garonzik S, Perera V, Garimella T and Humphreys WG (2018b) Further Studies to Support the Use of Coproporphyrin I and III as Novel Clinical Biomarkers for Evaluating the Potential for Organic Anion Transporting Polypeptide (OATP) 1B1 and OATP1B3 Inhibition. *Drug Metab Dispos*.

Shen H, Dai J, Liu T, Cheng Y, Chen W, Freeden C, Zhang Y, Humphreys WG, Marathe P and Lai Y (2016a) Coproporphyrins I and III as Functional Markers of OATP1B Activity: In Vitro and In Vivo Evaluation in Preclinical Species. *J Pharmacol Exp Ther* 357: 382-393.

Shen H, Liu T, Jiang H, Titsch C, Taylor K, Kandoussi H, Qiu X, Chen C, Sukrutharaj S, Kuit K, Mintier G, Krishnamurthy P, Fancher RM, Zeng J, Rodrigues AD, Marathe P and Lai Y (2016b) Cynomolgus Monkey as a Clinically Relevant Model to Study Transport Involving Renal Organic Cation Transporters: In Vitro and In Vivo Evaluation. *Drug Metab Dispos* 44: 238-249.

Shen H, Nelson DM, Oliveira RV, Zhang Y, McNaney CA, Gu X, Chen W, Su C, Reily MD, Shipkova PA, Gan J, Lai Y, Marathe P and Humphreys WG (2018c) Discovery and Validation of Pyridoxic Acid and Homovanillic Acid as Novel Endogenous Plasma

Downloaded from dmd.aspetjournals.org at ASPET Journals on April 18, 2024

DMD Fast Forward. Published on June 1, 2020 as DOI: 10.1124/dmd.120.090670
This article has not been copyedited and formatted. The final version may differ from this version.

Biomarkers of Organic Anion Transporter (OAT) 1 and OAT3 in Cynomolgus Monkeys. *Drug Metab Dispos* 46: 178-188.

Shen H, Su H, Liu T, Yao M, Mintier G, Li L, Fancher RM, Iyer R, Marathe P, Lai Y and Rodrigues AD (2015) Evaluation of rosuvastatin as an organic anion transporting polypeptide (OATP) probe substrate: in vitro transport and in vivo disposition in cynomolgus monkeys. *J Pharmacol Exp Ther* 353: 380-391.

Shen H, Wang L, Chen W, Menard K, Hong Y, Tian Y, Bonacorsi SJ, Humphreys WG, Lee FY and Gan J (2016c) Tissue distribution and tumor uptake of folate receptor-targeted epothilone folate conjugate, BMS-753493, in CD2F1 mice after systemic administration. *Acta Pharm Sin B* 6: 460-467.

Shen H, Yang Z, Mintier G, Han YH, Chen C, Balimane P, Jemal M, Zhao W, Zhang R, Kallipatti S, Selvam S, Sukrutharaj S, Krishnamurthy P, Marathe P and Rodrigues AD (2013) Cynomolgus monkey as a potential model to assess drug interactions involving hepatic organic anion transporting polypeptides: in vitro, in vivo, and in vitro-to-in vivo extrapolation. *J Pharmacol Exp Ther* 344: 673-685.

Shimizu Y, Naruto H, Ida S and Kohakura M (1981) Urinary coproporphyrin isomers in Rotor's syndrome: a study in eight families. *Hepatology* 1: 173-178.

Takahashi T, Ohtsuka T, Uno Y, Utoh M, Yamazaki H and Kume T (2016) Pre-incubation with cyclosporine A potentiates its inhibitory effects on pitavastatin uptake mediated by recombinantly expressed cynomolgus monkey hepatic organic anion transporting polypeptide. *Biopharm Drug Dispos* 37: 479-490.

Takahashi T, Ohtsuka T, Yoshikawa T, Tatekawa I, Uno Y, Utoh M, Yamazaki H and Kume T (2013) Pitavastatin as an in vivo probe for studying hepatic organic anion transporting polypeptide-mediated drug-drug interactions in cynomolgus monkeys. *Drug Metab Dispos* 41: 1875-1882.

Takahashi T, Uno Y, Yamazaki H and Kume T (2019) Functional characterization for polymorphic organic anion transporting polypeptides (OATP/SLCO1B1, 1B3, 2B1) of monkeys recombinantly expressed with various OATP probes. *Biopharm Drug Dispos* 40: 62-69.

Downloaded from dmd.aspetjournals.org at ASPET Journals on April 18, 2024

DMD Fast Forward. Published on June 1, 2020 as DOI: 10.1124/dmd.120.090670
This article has not been copyedited and formatted. The final version may differ from this version.

Takehara I, Watanabe N, Mori D, Ando O and Kusuhara H (2019) Effect of Rifampicin on the Plasma Concentrations of Bile Acid-O-Sulfates in Monkeys and Human Liver-Transplanted Chimeric Mice With or Without Bile Flow Diversion. *J Pharm Sci* 108: 2756-2764.

Takehara I, Yoshikado T, Ishigame K, Mori D, Furihata KI, Watanabe N, Ando O, Maeda K, Sugiyama Y and Kusuhara H (2018) Comparative Study of the Dose-Dependence of OATP1B Inhibition by Rifampicin Using Probe Drugs and Endogenous Substrates in Healthy Volunteers. *Pharm Res* 35: 138.

Thakare R, Gao H, Kosa RE, Bi YA, Varma MV, Cerny M, Sharma R, Kuhn M, Huang B, Liu Y, Yu A, Walker GS, Niosi M, Tremaine LM, Alnouti Y and Rodrigues AD (2017a) Leveraging of Rifampicin-Dosed Cynomolgus Monkeys to Identify Bile Acid 3-O-Sulfate Conjugates as Potential Novel Biomarkers for Organic Anion-Transporting Polypeptides. *Drug Metab Dispos*.

Thakare R, Gao H, Kosa RE, Bi YA, Varma MVS, Cerny MA, Sharma R, Kuhn M, Huang B, Liu Y, Yu A, Walker GS, Niosi M, Tremaine L, Alnouti Y and Rodrigues AD (2017b) Leveraging of Rifampicin-Dosed Cynomolgus Monkeys to Identify Bile Acid 3-O-Sulfate Conjugates as Potential Novel Biomarkers for Organic Anion-Transporting Polypeptides. *Drug Metab Dispos* 45: 721-733.

Tomita Y, Maeda K and Sugiyama Y (2013) Ethnic variability in the plasma exposures of OATP1B1 substrates such as HMG-CoA reductase inhibitors: a kinetic consideration of its mechanism. *Clin Pharmacol Ther* 94: 37-51.

Ufuk A, Kosa RE, Gao H, Bi YA, Modi S, Gates D, Rodrigues AD, Tremaine LM, Varma MVS, Houston JB and Galetin A (2018) In Vitro-In Vivo Extrapolation of OATP1B-Mediated Drug-Drug Interactions in Cynomolgus Monkey. *J Pharmacol Exp Ther* 365: 688-699.

Wang L, Prasad B, Salphati L, Chu X, Gupta A, Hop CE, Evers R and Unadkat JD (2015) Interspecies variability in expression of hepatobiliary transporters across human, dog, monkey, and rat as determined by quantitative proteomics. *Drug Metab Dispos* 43: 367-374.

Wilson J, Grant PJ, Davies JA, Boothby M, Gaffney PJ and Prentice CR (1988) The relationship between plasma vasopressin and changes in coagulation and fibrinolysis during hip surgery. *Thromb Res* 51: 439-445.

Wolkoff AW, Wolpert E, Pascasio FN and Arias IM (1976) Rotor's syndrome. A distinct inheritable pathophysiologic entity. *Am J Med* 60: 173-179.

Downloaded from dmd.aspetjournals.org at ASPET Journals on April 18, 2024

DMD Fast Forward. Published on June 1, 2020 as DOI: 10.1124/dmd.120.090670
This article has not been copyedited and formatted. The final version may differ from this version.

Yee SW, Giacomini MM, Shen H, Humphreys WG, Horng H, Brian W, Lai Y, Kroetz DL and Giacomini KM (2019) Organic Anion Transporter Polypeptide 1B1 Polymorphism Modulates the Extent of Drug-Drug Interaction and Associated Biomarker Levels in Healthy Volunteers. *Clin Transl Sci* 12: 388-399.

Yoshida K, Guo C and Sane R (2018) Quantitative Prediction of OATP-Mediated Drug-Drug Interactions With Model-Based Analysis of Endogenous Biomarker Kinetics. *CPT Pharmacometrics Syst Pharmacol* 7: 517-524.

Yoshikado T, Toshimoto K, Maeda K, Kusuhara H, Kimoto E, Rodrigues AD, Chiba K and Sugiyama Y (2018) PBPK Modeling of Coproporphyrin I as an Endogenous Biomarker for Drug Interactions Involving Inhibition of Hepatic OATP1B1 and OATP1B3. *CPT Pharmacometrics Syst Pharmacol* 7: 739-747.

Yu J, Petrie ID, Levy RH and Ragueneau-Majlessi I (2019) Mechanisms and Clinical Significance of Pharmacokinetic-Based Drug-Drug Interactions with Drugs Approved by the U.S. Food and Drug Administration in 2017. *Drug Metab Dispos* 47: 135-144.

Zhang Y, Panfen E, Fancher M, Sinz M, Marathe P and Shen H (2019) Dissecting the Contribution of OATP1B1 to Hepatic Uptake of Statins Using the OATP1B1 Selective Inhibitor Estropipate. *Mol Pharm* 16: 2342-2353.

Downloaded from dmd.aspetjournals.org at ASPET Journals on April 18, 2024

DMD Fast Forward. Published on June 1, 2020 as DOI: 10.1124/dmd.120.090670
This article has not been copyedited and formatted. The final version may differ from this version.

Footnotes

Reprint requests:

- **Hong Shen**, Route 206 & Province Line Road., Bristol-Myers Squibb Company, Princeton, NJ 08543-4000. Telephone: (609) 252-4509; E-mail: hong.shen1@bms.com;

- This study is supported by Bristol-Myers Squibb Company.

Downloaded from dmd.aspetjournals.org at ASPET Journals on April 18, 2024

DMD Fast Forward. Published on June 1, 2020 as DOI: 10.1124/dmd.120.090670
This article has not been copyedited and formatted. The final version may differ from this version.

Figure Legends

Figure 1. Plasma concentration of octadeuterated coproporphyrin I (CPI-d8) from 0 to 24 h (A) and 0 to 5 h (B) in cynomolgus monkeys (n = 3) after intravenous (IV) infusion of 0.1 mg/kg CPI-d8 for 10 min and oral (PO) administration of 0.2 mg/kg CPI-d8 alone or in combination with CsA (PO, 100 mg/kg). In the coadministration groups, a CPI-d8 solution was administered to each animal 60 min after CsA administration. Data are expressed as mean and standard deviation (mean ± SD).

Figure 2. Plasma concentration (A), maximum plasma concentration (C_{max}) (B), area under the plasma concentration-time curve (*AUC*) (C) of Cyclosporin A (CsA) in cynomolgus monkeys (n = 3) after oral drug administration at different doses: 4, 20, and 100 mg/kg. Data are expressed as mean and standard deviation (mean ± SD).

Figure 3. Plasma concentrations of CPI (A), CPIII (B), and CPI-d8 (C) over time in cynomolgus monkeys (n = 3) after a single intravenous dose of 0.1 mg/kg CPI-d8 with and without CsA given as an oral dose of 4, 20, or 100 mg/kg. In the coadministration groups, a CPI-d8 solution (0.1 mg/kg) was administered orally to each monkey 60 min after CsA administration (100 mg/kg; PO). Data are expressed as mean and standard deviation (mean ± SD). Inset depicts the same data from 0 to 1 h.

Figure 4. Correlation between the fold changes in the area under the plasma concentration-time curves from time of CsA administration up to the time of the last quantifiable concentration (*AUCR*) of CPI, CPIII, and CPI-d8 in cynomolgus monkeys.

Downloaded from dmd.aspetjournals.org at ASPET Journals on April 18, 2024

DMD Fast Forward. Published on June 1, 2020 as DOI: 10.1124/dmd.120.090670
This article has not been copyedited and formatted. The final version may differ from this version.

Figure 5. Correlation between CsA maximum plasma concentration (C_{max}) (A) or area under the concentration–time curve from time of administration up to 24 h ($AUC_{(0\text{-}24h)}$) (B) and *AUCR* values of CPI, CPIII, and CPI-d8 after the administration of CsA in cynomolgus monkeys.

Figure 6. Plasma concentrations of CPI and CPIII at 1, 5, and 24 h after administration of a single intravenous dose of 3.9 mg/kg metformin (MFM) (closed squares and triangles, respectively) and coadministration of intravenous dose of 0.5 mg/kg pyrimethamine (PYR) and MFM (open squares and triangles, respectively. Data are expressed as mean and standard deviation (mean ± SD).

Downloaded from dmd.aspetjournals.org at ASPET Journals on April 18, 2024

DMD Fast Forward. Published on June 1, 2020 as DOI: 10.1124/dmd.120.090670
This article has not been copyedited and formatted. The final version may differ from this version.

Table 1. Cynomolgus Monkey CPI-d8 Dosing and Administration Route Groups

Group	Pretreatment	CPI-d8 Dose[a]	PI-d8 Administration Route	Replicate (n)
1	None	0.2 mg/kg	PO	3
2	None	0.1 mg/kg	IV	3
3	4 mg/kg CsA, PO	0.1 mg/kg	IV	3
4	20 mg/kg CsA, PO	0.1 mg/kg	IV	6[b]
5	100 mg/kg CsA, PO	0.1 mg/kg	IV	3
6	100 mg/kg CsA, PO	0.2 mg/kg	PO	3

Downloaded from dmd.aspetjournals.org at ASPET Journals on April 18, 2024

DMD Fast Forward. Published on June 1, 2020 as DOI: 10.1124/dmd.120.090670
This article has not been copyedited and formatted. The final version may differ from this version.

Table 1 Legend:

[a]In the coadministration groups (i.e., Groups 3, 4, 5, and 6, a CPI-d8 solution was administered to each monkey 60 min after CsA administration

[b]A crossover study design was used and the same three male cynomolgus monkeys were dosed over a series of six treatments with a 1-week washout between treatments (n = 3). One exception was the Group 4 that was repeated due to dosing mistake (n = 6).

IV, intravenous administration; PO, oral administration.

Downloaded from dmd.aspetjournals.org at ASPET Journals on April 18, 2024

DMD Fast Forward. Published on June 1, 2020 as DOI: 10.1124/dmd.120.090670
This article has not been copyedited and formatted. The final version may differ from this version.

Table 2. Mean Pharmacokinetic Parameters of CPI-d8 in Cynomolgus Monkeys after A Single 10-min Intravenous Infusion of 0.1 mg/kg CPI-d8 alone, A Single Oral Doses of 0.2 mg/kg CPI-d8 alone, and Combination of CsA (PO, 100 mg/kg) with CPI-d8

Pharmacokinetic Parameter	Intravenous		Oral	
	CPI-d8 Alone	With CsA	CPI-d8 Alone	With CsA
C_{max} (nM)	NA	NA	1.1 ± 0.5	7.2 ± 7.5
T_{max} (h)	NA	NA	1.5 ± 1.3	0.3 ± 0.4
$AUC_{0\text{-}24h}$ (nM•h)	188 ± 31.4	2102 ± 1645*	9.8 ± 3.0	21.1 ± 8.3
AUC_{TOT} (nM•h)	189 ± 31.5	2128 ± 1686*	11.5 ± 3.4	25.0 ± 7.2
Vd_{SS} (L/kg)	0.57 ± 0.10	0.24 ± 0.13**	NA	NA
CL_{TOT} (mL/min/kg)	10.1 ± 1.7	1.3 ± 0.9**	NA	NA
$T_{1/2}$ (h)	7.6 ± 0.5	3.3 ± 1.1*	11.2 ± 4.6	8.6 ± 3.1
F (%)	NA	NA	3.2 ± 1.7	0.8 ± 0.6

Downloaded from dmd.aspetjournals.org at ASPET Journals on April 18, 2024

DMD Fast Forward. Published on June 1, 2020 as DOI: 10.1124/dmd.120.090670
This article has not been copyedited and formatted. The final version may differ from this version.

Table 2 Legend:

Data are presented as mean ± SD (n = 3 monkeys). CPI-d8 was administered 60 min after CsA administration (PO, 100 mg/kg). The pharmacokinetic parameters were determined as indicated under *Materials and Methods*.

NA, not applicable.

Statistics were conducted by two-sided paired Student's *t* test. * $p < 0.05$ and ** $p < 0.01$ compared with the CsA alone administration group.

Downloaded from dmd.aspetjournals.org at ASPET Journals on April 18, 2024

DMD Fast Forward. Published on June 1, 2020 as DOI: 10.1124/dmd.120.090670
This article has not been copyedited and formatted. The final version may differ from this version.

Table 3. Mean Pharmacokinetic Parameters of CsA in Cynomolgus Monkeys after A Single Oral Dose of 4, 20, or 100 mg/kg CsA

Pharmacokinetic Parameters	CsA Dose		
	4 mg/kg (n = 3)	20 mg/kg (n = 6)	100 mg/kg (n = 6)
Blood $AUC_{0\text{-}24h}$ (μM•h)	2.7 ± 0.6	10.5 ± 7.5	26.6 ± 4.1***;£
Blood C_{max} (μM)	0.19 ± 0.04	2.5 ± 1.6*	3.8 ± 2.3*
T_{max} (h)	2.7 ± 0.6	2.3 ± 2.5	4.0 ± 1.7
$T_{1/2}$ (h)	5.2 ± 1.6	6.2 ± 1.7	9.1 ± 2.0*

Downloaded from dmd.aspetjournals.org at ASPET Journals on April 18, 2024

DMD Fast Forward. Published on June 1, 2020 as DOI: 10.1124/dmd.120.090670
This article has not been copyedited and formatted. The final version may differ from this version.

Table 3 Legend:

Data are presented as mean ± SD (n = 3, 6, and 6 monkeys at doses of 4, 20, and 100 mg/kg, respectively). The pharmacokinetic parameters were determined as indicated under *Materials and Methods*.

Statistics were conducted by one-way ANOVA followed by Dunnett's multiple comparison method. *$p < 0.05$ and *** $p < 0.001$ compared with the 4 mg/kg CsA group, and $^{£}p < 0.05$ compared with the 20 mg/kg CsA group.

Downloaded from dmd.aspetjournals.org at ASPET Journals on April 18, 2024

DMD Fast Forward. Published on June 1, 2020 as DOI: 10.1124/dmd.120.090670
This article has not been copyedited and formatted. The final version may differ from this version.

Table 4. Mean Systemic Exposures of CP in Cynomolgus Monkeys after A Single 10-min Infusion of CPI-d8 (0.1 mg/kg) with Increasing Doses of CsA (PO, 4, 20, and 100 mg/kg)

Analyte	Pharmacokinetic Parameters	Oral CsA Dose			
		Vehicle	4 mg/kg	20 mg/kg	100 mg/kg
CPI-d8[a]	$AUC_{0\text{-}24h}$ (nM•h)	188 ± 31.4	345 ± 88**	1142 ± 432**	2102 ± 1645*
	AUCR	1.0	1.8 ± 0.3**	6.2 ± 2.5**	10.5 ± 6.8*
CPI[b]	$AUC_{0\text{-}24h}$ (nM•h)	8.9 ± 0.7	9.7 ± 1.9	12.7 ± 3.2	39.6 ± 21.0*
	AUCR	1.0	1.1 ± 0.3	1.4 ± 0.3*	4.4 ± 2.1*
	C_{max} (nM)	0.58 ± 0.11	0.58 ± 0.10	1.47 ± 0.46	2.84 ± 0.94
	$C_{max}R$	1.0	1.2 ± 0.16	3.0 ± 0.9**	5.8 ± 1.9**
CPIII[b]	$AUC_{0\text{-}24h}$ (nM•h)	3.0 ± 0.6	2.7 ± 0.7	4.6 ± 2.5	11.6 ± 8.0
	AUCR	1.0	1.1 ± 0.3	1.8 ± 0.9	4.6 ± 3.0
	C_{max} (nM)	0.19 ± 0.07	0.21 ± 0.08	0.48 ± 0.16*	0.86 ± 0.37*
	$C_{max}R$	1.0	1.6 ± 0.9	3.8 ± 1.7*	6.9 ± 3.7*

Downloaded from dmd.aspetjournals.org at ASPET Journals on April 18, 2024

DMD Fast Forward. Published on June 1, 2020 as DOI: 10.1124/dmd.120.090670
This article has not been copyedited and formatted. The final version may differ from this version.

Table 4 Legend:

Data are presented as mean ± SD. The pharmacokinetic parameters were determined as indicated under *Materials and Methods*.

[a] n = 3, 3, 6, and 3 monkeys at doses of 0 (vehicle), 4, 20, and 100 mg/kg, respectively.

[b] n = 6, 3, 6, and 6 monkeys at doses of 0 (vehicle), 4, 20, and 100 mg/kg, respectively.

AUCR and C_{max}R, fold changes in AUC and C_{max} of CP dosed with CsA compared to vehicle control.

Statistics were conducted by one-way ANOVA followed by Dunnett's multiple comparison method. *$p < 0.05$, **$p < 0.01$, and ***$p < 0.001$ compared with the vehicle group.

Downloaded from dmd.aspetjournals.org at ASPET Journals on April 18, 2024

DMD Fast Forward. Published on June 1, 2020 as DOI: 10.1124/dmd.120.090670
This article has not been copyedited and formatted. The final version may differ from this version.

Table 5. Prediction of the DDI Caused by CsA in Cynomolgus Monkeys Using Mechanistic Static Model

Treatment	DDI Prediction				Observed CPI-d8 Fold Change	Observed CPI Fold Change	Observed CPIII Fold Change
	cOATP1B1		cOATP1B3				
	IC_{50} (µM)	*AUCR*	IC_{50} (µM)	*AUCR*			
4 mg/kg CsA	0.28	1.58	0.25	1.65	1.8	1.1	1.1
20 mg/kg CsA	0.28	4.06	0.25	4.42	6.2	1.4	1.8
100 mg/kg CsA	0.28	15.4	0.25	17.1	10.5	4.4	4.6

Downloaded from dmd.aspetjournals.org at ASPET Journals on April 18, 2024

DMD Fast Forward. Published on June 1, 2020 as DOI: 10.1124/dmd.120.090670
This article has not been copyedited and formatted. The final version may differ from this version.

Table 5 Legend:

IC$_{50}$, concentration required to inhibit transport by 50%; *AUCR*, predicted ratio of victim drug *AUC* in the presence and absence of CsA of OATP1B1 and OATP1B3 using the static mechanistic model recommended by US Food and Drug Administration ($AUCR = 1 + I_{in,max,u}/IC_{50}$), where $I_{in,max,u}$ is the maximum unbound hepatic inlet concentration after oral CsA administration

f_u, fraction absorbed (f_a), and intestinal availability (f_g) data of CsA obtained from previous reports (Awni et al., 1989, Drewe et al., 1992, Mueller et al., 1994), and the values in humans are assumed to those in cynomolgus monkeys

Downloaded from dmd.aspetjournals.org at ASPET Journals on April 18, 2024

DMD Fast Forward. Published on June 1, 2020 as DOI: 10.1124/dmd.120.090670
This article has not been copyedited and formatted. The final version may differ from this version.

Table 6. Mean Systemic Exposures of CP in Cynomolgus Monkeys after A Single Intravenous Dose of 2 mg/kg FSM alone, PROB alone (IV, 40 mg/kg), and PROB with FSM

Analyte	Pharmacokinetic Parameters	Intravenous PROB Dose		
		FSM Alone	PROB Alone	FSM with PROB
CPI	$AUC_{0\text{-}24h}$ (nM•h)	3.8 ± 1.1	2.9 ± 0.5	3.3 ± 1.1
	AUCR	1.0	0.78 ± 0.09	0.89 ± 0.15
	C_{max} (nM)	0.78 ± 0.26	0.56 ± 0.12	0.64 ± 0.26
	$C_{max}R$	1.0	0.75 ± 0.13	0.84 ± 0.25
CPIII	$AUC_{0\text{-}7h}$ (nM•h)	0.76 ± 0.22	1.05 ± 0.19	1.35 ± 0.50
	AUCR	1.0	1.5 ± 0.4	1.9 ± 0.7
	C_{max} (nM)	0.14 ± 0.04	0.25 ± 0.04*	0.34 ± 0.11
	$C_{max}R$	1.0	1.9 ± 0.5	2.5 ± 0.8

Downloaded from dmd.aspetjournals.org at ASPET Journals on April 18, 2024

DMD Fast Forward. Published on June 1, 2020 as DOI: 10.1124/dmd.120.090670
This article has not been copyedited and formatted. The final version may differ from this version.

Table 6 Legend:

Data are presented as mean ± SD (n = 3). The pharmacokinetic parameters were determined as indicated under *Materials and Methods*.

AUCR and C_{max}R, fold changes in *AUC* and C_{max} of CP dosed with PROB alone and with FSM compared to FSM group.

Statistics were conducted by one-way ANOVA followed by Dunnett's multiple comparison method. *$p < 0.05$ compared with the FSM group.

Downloaded from dmd.aspetjournals.org at ASPET Journals on April 18, 2024

DMD Fast Forward. Published on June 1, 2020 as DOI: 10.1124/dmd.120.090670
This article has not been copyedited and formatted. The final version may differ from this version.

Table 7. Tissue Concentration of [^{3}H]CPI Determined by QWBA in Mice after A Single Intravenous Dose of 0.04 mg/kg [^{3}H]CPI (5 mCi/kg) alone and [^{3}H]CPI with RIF (PO, 100 mg/kg) (n = 8 for each group and n =2 for each time point)

IV [^{3}H]CPI Dose	Tissue	Concentration (nCi [^{3}H]CPI/g)			
		2 min	20 min	3 h	24 h
[^{3}H]CPI Alone	Blood	90	110	0	0
	Brain	0	0	0	0
	Liver	140	360	0	0
	Lung	90	120	0	0
	Kidney	1972	80	0	0
	Intestine	0	5850	4110	0
[^{3}H]CPI with RIF	Blood	150	300	0	0
	Brain	0	0	0	0
	Liver	80	150	50	0
	Lung	250	210	0	0
	Kidney	50	300	30	0
	Intestine	10	20	1350	0

Downloaded from dmd.aspetjournals.org at ASPET Journals on April 18, 2024

DMD Fast Forward. Published on June 1, 2020 as DOI: 10.1124/dmd.120.090670
This article has not been copyedited and formatted. The final version may differ from this version.

Table 7 Legend:

[^{3}H]CPI was administered intravenously 60 min after RIF administration (PO, 100 mg/kg) in male C57BL6 mice. The QWBA was performed as indicated under *Materials and Methods*.

Downloaded from dmd.aspetjournals.org at ASPET Journals on April 18, 2024

DMD Fast Forward. Published on June 1, 2020 as DOI: 10.1124/dmd.120.090670
This article has not been copyedited and formatted. The final version may differ from this version.

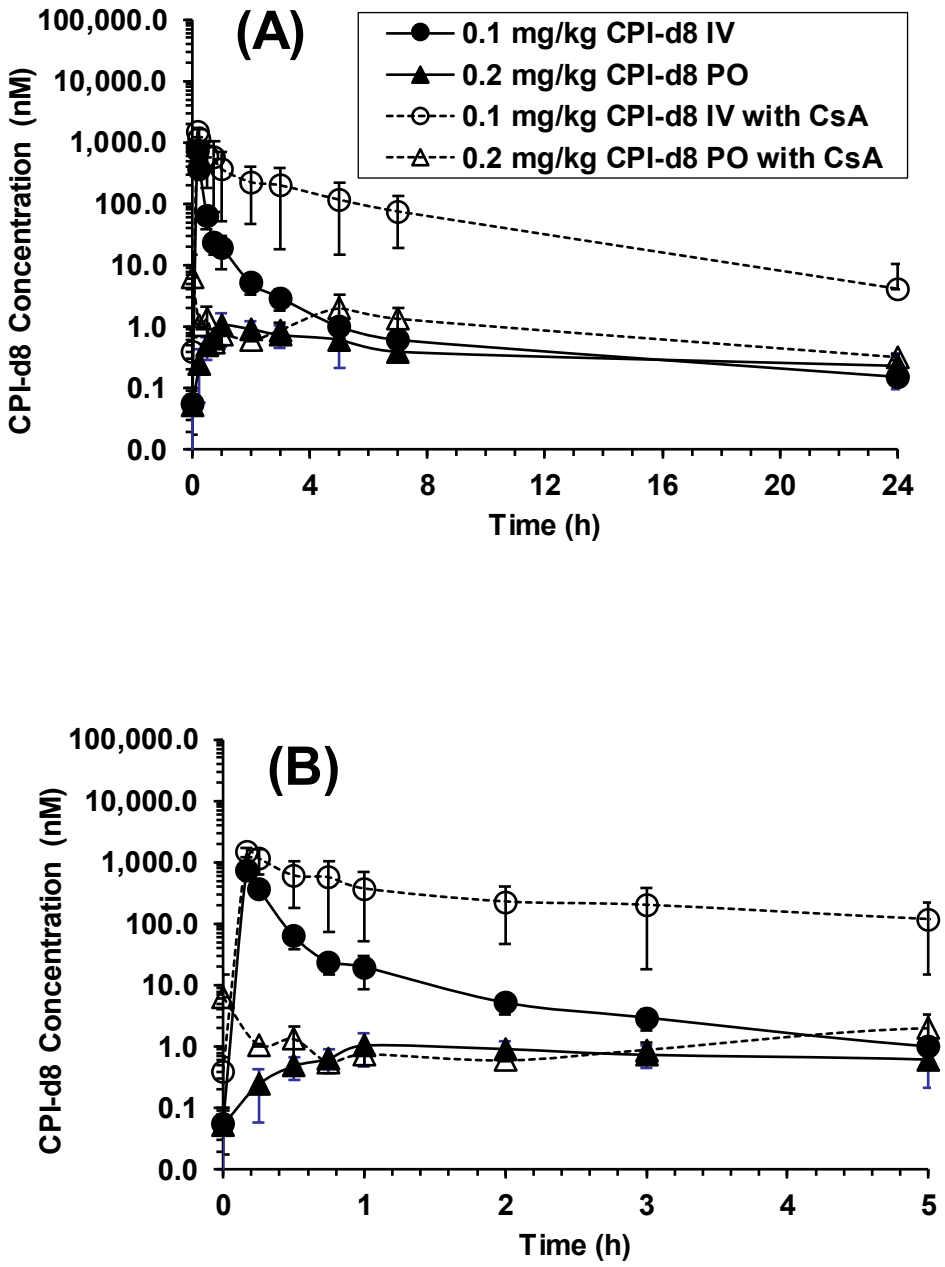

Figure 1

Downloaded from dmd.aspetjournals.org at ASPET Journals on April 18, 2024

DMD Fast Forward. Published on June 1, 2020 as DOI: 10.1124/dmd.120.090670
This article has not been copyedited and formatted. The final version may differ from this version.

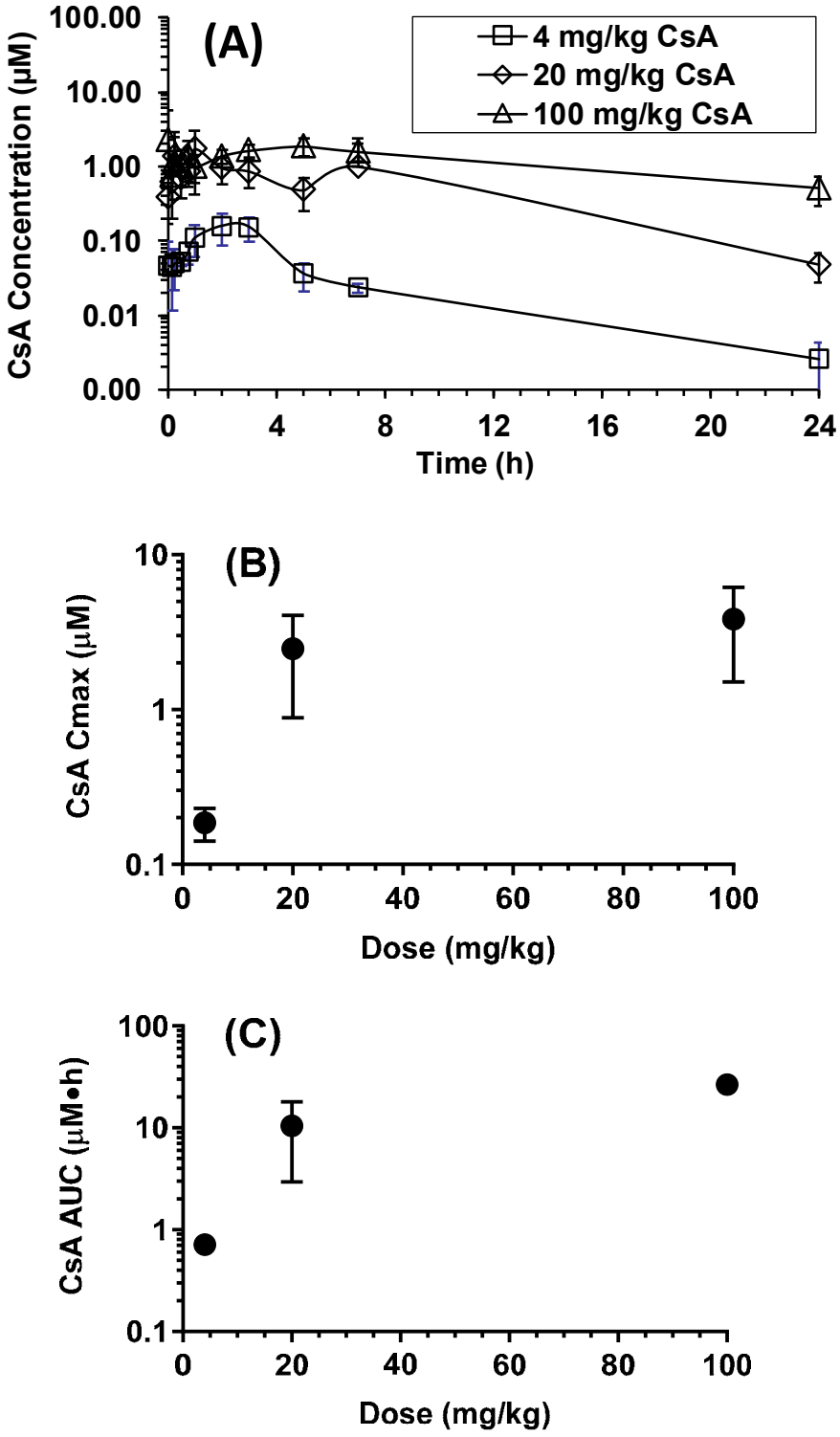

Figure 2

Downloaded from dmd.aspetjournals.org at ASPET Journals on April 18, 2024

DMD Fast Forward. Published on June 1, 2020 as DOI: 10.1124/dmd.120.090670
This article has not been copyedited and formatted. The final version may differ from this version.

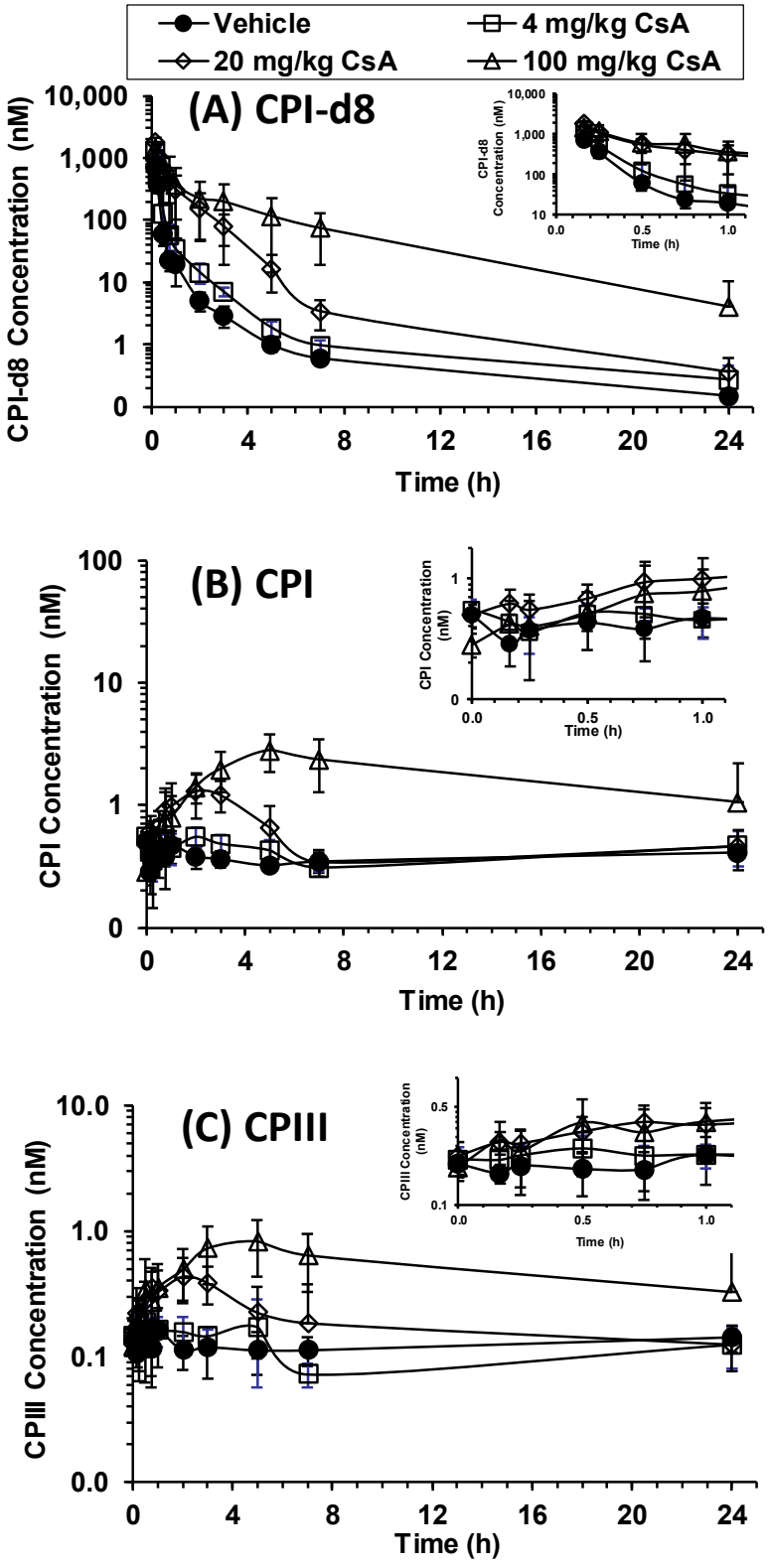

Figure 3

Downloaded from dmd.aspetjournals.org at ASPET Journals on April 18, 2024

DMD Fast Forward. Published on June 1, 2020 as DOI: 10.1124/dmd.120.090670
This article has not been copyedited and formatted. The final version may differ from this version.

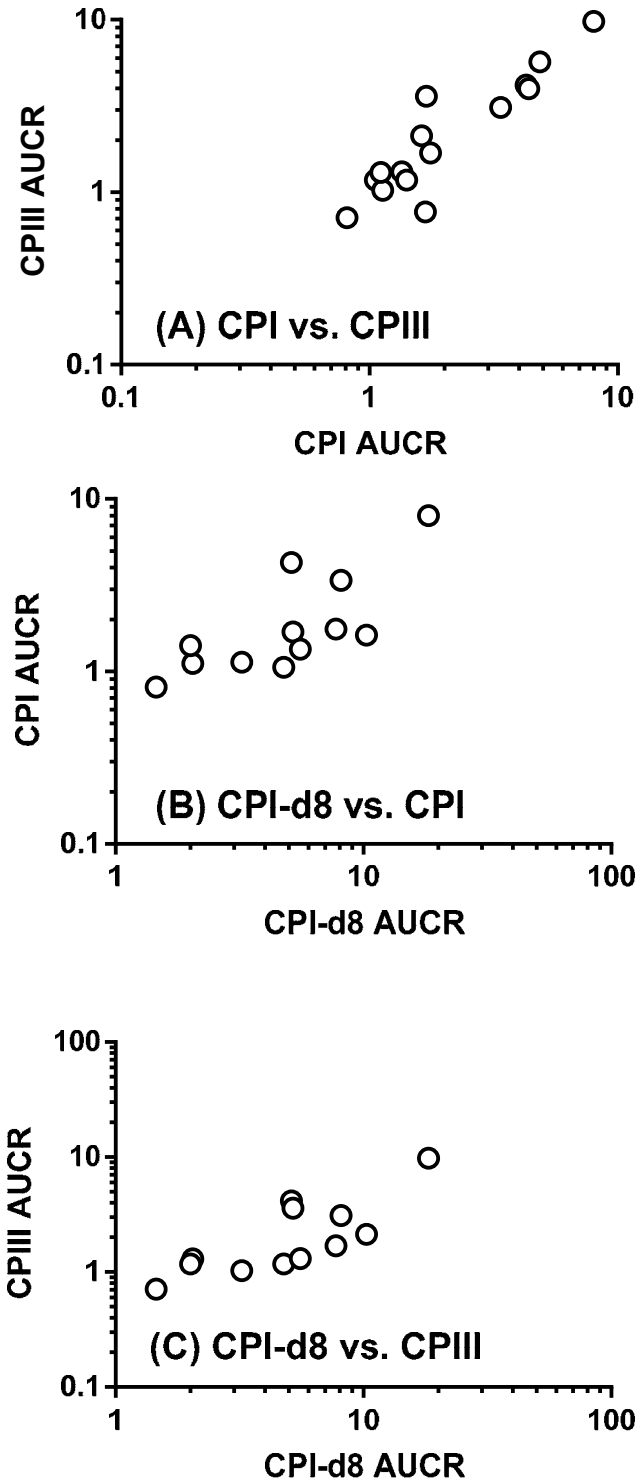

Figure 4

Downloaded from dmd.aspetjournals.org at ASPET Journals on April 18, 2024

DMD Fast Forward. Published on June 1, 2020 as DOI: 10.1124/dmd.120.090670
This article has not been copyedited and formatted. The final version may differ from this version.

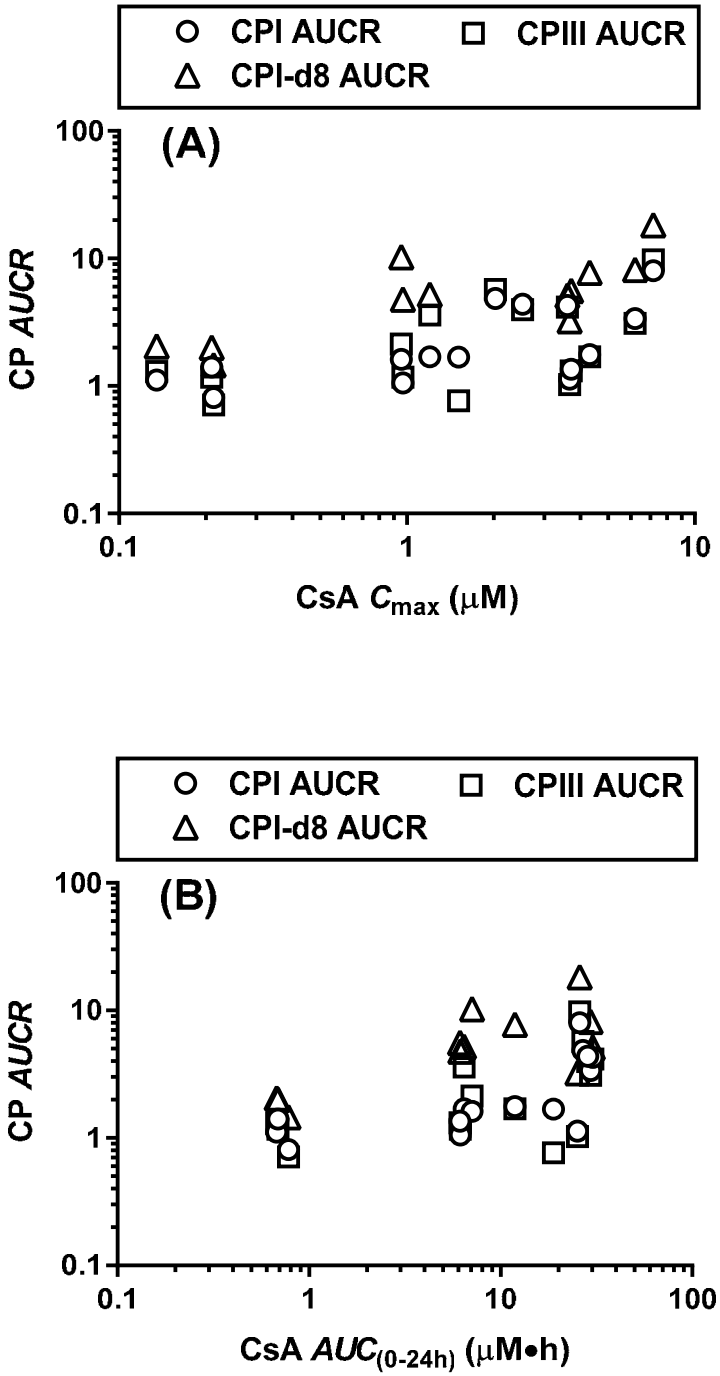

Figure 5

Downloaded from dmd.aspetjournals.org at ASPET Journals on April 18, 2024

DMD Fast Forward. Published on June 1, 2020 as DOI: 10.1124/dmd.120.090670
This article has not been copyedited and formatted. The final version may differ from this version.

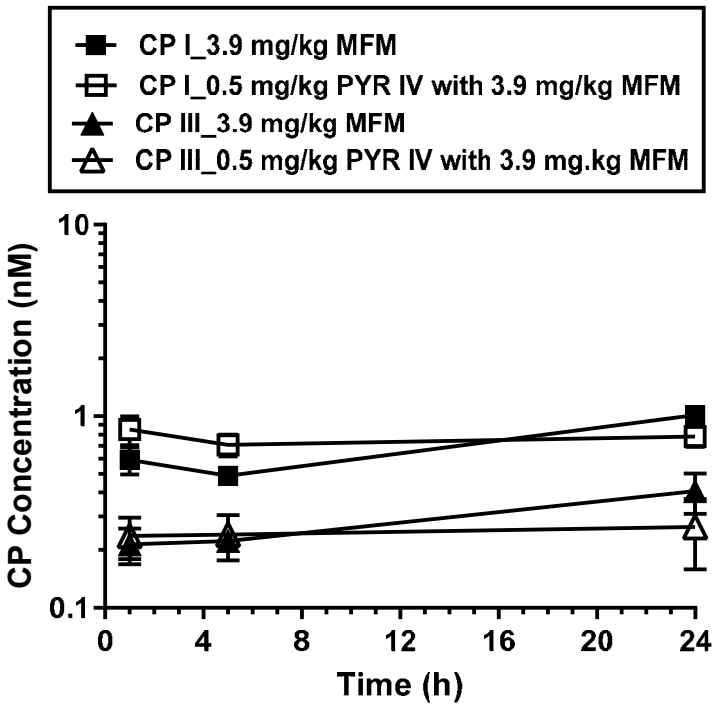

Figure 6

Downloaded from dmd.aspetjournals.org at ASPET Journals on April 18, 2024

Supplementary Figures and Tables

Absorption and Disposition of Coproporphyrin I (CPI) in Cynomolgus Monkeys and Mice: Pharmacokinetic Evidence to Support the Use of CPI to Inform the Potential for OATP Inhibition

Xiaomei Gu, Lifei Wang, Jinping Gan, R. Marcus Fancher, Yuan Tian, Yang Hong, Yurong Lai, Michael Sinz, and Hong Shen

Departments of Metabolism and Pharmacokinetics (X.G., L.W., J.G., R.M.F., Y.L., M.S., and H.S.) and Radiochemistry (Y.H and Y.T.), Bristol-Myers Squibb Company, Route 206 & Province Line Road, Lawrenceville, NJ 08543

Supplementary Figure 1

Molecular Structures of CPI-d8, CPIII-d8, and [^{3}H]CPI

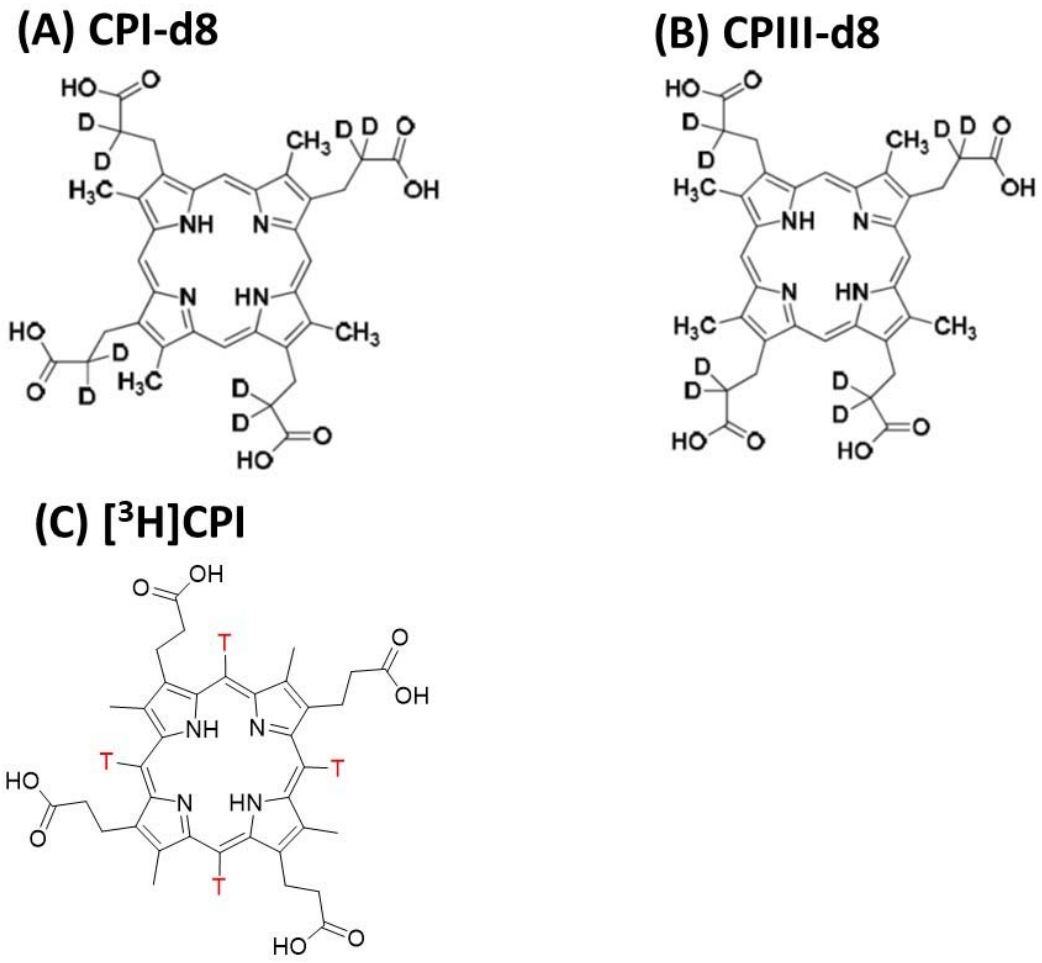

Supplementary Figure 2

Plasma concentrations of CPI (A) and CPIII (B) over time in cynomolgus monkeys (n = 3) after administration of a single intravenous dose of 2 mg/kg furosemide (FSM) (closed circles), a single intravenous dose of 40 mg probenecid (PROB) (open squares), and PROB coadministration with FSM (open diamonds). Data are expressed as mean and standard deviation (mean ± SD). Inset depicts the same data from 0 to 1 h.

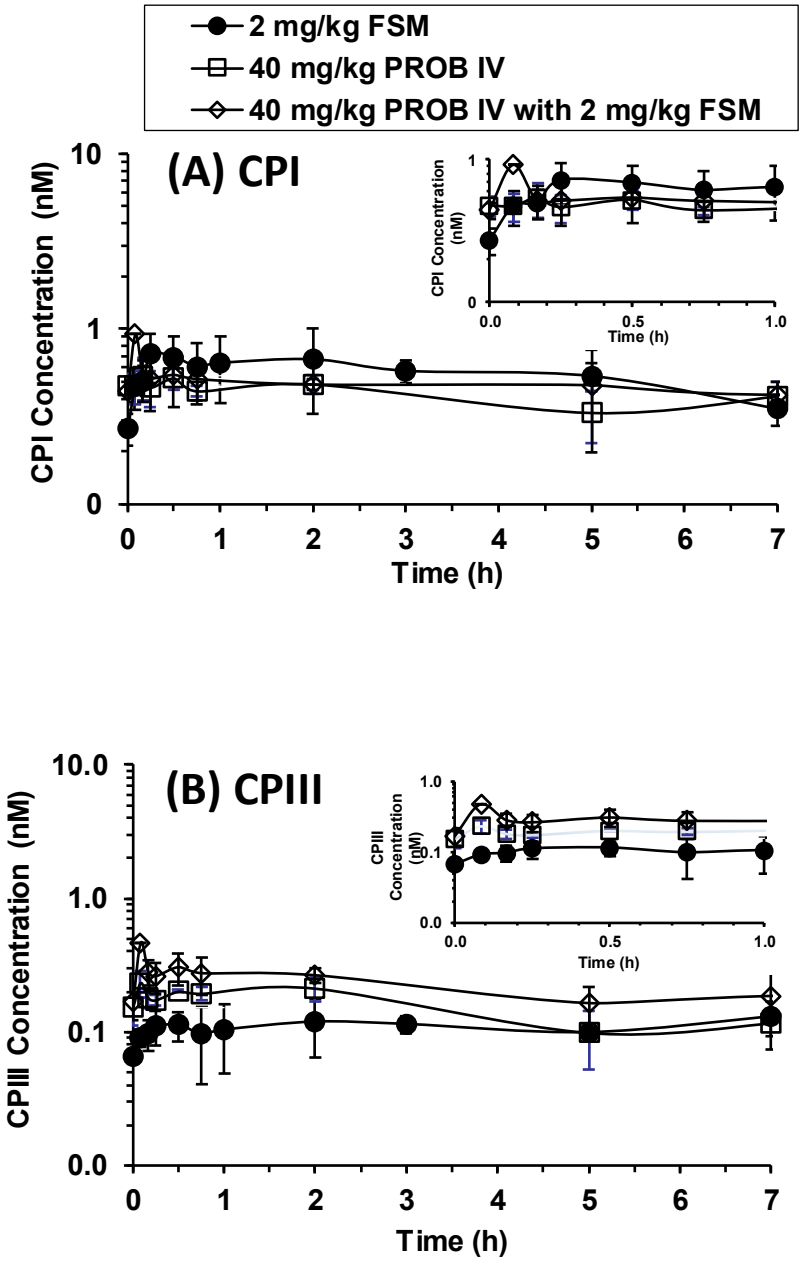

Supplementary Figure 3

Quantitative whole-body autoradiography (QWBA) after intravenous administration of 0.04 mg/kg [3H]CPI in normal 57BL6 mice. Male 57BL6 mice were administered intravenously with [3H]CPI at 0.04 mg/kg alone (A, C, and E) and with rifampin (RIF) given as an oral dose of (100 mg/kg; n = 2) (B, E, and F), and then were frozen for QWBA at 2 min, 20 min, 3 h, and 24 h after [3H]CPI administration. Images were contrast-enhanced for display purposes only.